ERDC/CERL TR-19-15

Construction Engineering Research Laboratory

US Army Corps of Engineers®
Engineer Research and Development Center

ERDC
ENGINEER RESEARCH & DEVELOPMENT CENTER

DoD Corrosion Prevention and Control Program

Rehabilitation of Deteriorated Wood Railroad Ties Using Inorganic Polymers

Final Report on Project F17-AR03

Ghassan K. Al-Chaar, Kaushik Sankar, and Waltraud M. Kriven

August 2019

Approved for public release; distribution is unlimited.

The U.S. Army Engineer Research and Development Center (ERDC) solves the nation's toughest engineering and environmental challenges. ERDC develops innovative solutions in civil and military engineering, geospatial sciences, water resources, and environmental sciences for the Army, the Department of Defense, civilian agencies, and our nation's public good. Find out more at www.erdc.usace.army.mil.

To search for other technical reports published by ERDC, visit the ERDC online library at http://acwc.sdp.sirsi.net/client/default.

Rehabilitation of Deteriorated Wood Railroad Ties Using Inorganic Polymers

Final Report on Project F17-AR03

Ghassan K. Al-Chaar

Construction Engineering Research Laboratory
U.S. Army Engineer Research and Development Center
2902 Newmark Drive
Champaign, IL 61822

Kaushik Sankar and Waltraud M. Kriven

University of Illinois at Urbana-Champaign
Department of Materials Science and Engineering
1304 W Green Street
Urbana, IL 61801

Final report

Approved for public release; distribution is unlimited.

Prepared for Office of the Secretary of Defense (OUSD(A&S))
3090 Defense Pentagon
Washington, DC 20301-3090

Under Project F17-AR03, "Rehabilitation of Deteriorated Wood Railroad Ties Using Inorganic Polymers"

Abstract

The U.S. Army owns and maintains about 1,900 miles of railroad track configured as short lines for mission-required on military installations where ordnance and other heavy freight must be moved in quantity onsite, or to connect with the national railroad network for long-distance transport. Almost all of crossties used in these rail lines are made of creosote-treated wood to support the rails. Wood offers several advantages in terms of life-cycle costs and structural suitability. Chemical treatment of wood ties extends their life cycles, but service life is still finite due to rot, consumption by insects, and other stressors. The removal and replacement of failed wood ties is costly, time-consuming, and disruptive to rail operations. Furthermore, the residual preservative chemicals also create a costly disposal problem.

This report describes the development of a cementitious geopolymer material based on slag-fly ash binder mixtures formulated with properties making it suitable for use as a tough, affordable in situ tie-rehabilitation material. Two candidate formulations were validated in lab experiments as easy to prepare onsite, and demonstrating excellent flowability with good compressive and flexural strength. Field demonstrations are still required to validate rehabilitation procedures and performance characteristics in Army rail line operations.

DISCLAIMER: The contents of this report are not to be used for advertising, publication, or promotional purposes. Citation of trade names does not constitute an official endorsement or approval of the use of such commercial products. All product names and trademarks cited are the property of their respective owners. The findings of this report are not to be construed as an official Department of the Army position unless so designated by other authorized documents.

DESTROY THIS REPORT WHEN NO LONGER NEEDED. DO NOT RETURN IT TO THE ORIGINATOR.

Contents

Abstract ii

Figures and Tables v

Unit Conversion Factors vii

Preface viii

1 Introduction 1
- 1.1 Problem statement 1
- 1.2 Objectives 2
- 1.3 Approach 2
- 1.4 Metrics 3
- 1.5 Scope of execution 4

2 Technical Investigation 5
- 2.1 Technology overview 5
- 2.2 AREMA track design standards 6
- 2.3 Candidate field test sites 10
- 2.4 Inorganic polymer tests 11
  - *2.4.1 Compression 11*
  - *2.4.2 Flexure 11*
  - *2.4.3 Shrinkage 11*
  - *2.4.4 Durability 11*
  - *2.4.5 Setting time 12*
- 2.5 Structural testing of repaired ties 13

3 Results 14
- 3.1 Binder, mortar, and concrete results 14
  - *3.1.1 Material nomenclature and compositions 14*
  - *3.1.2 Setting time 16*
  - *3.1.3 Microstructural analysis 18*
  - *3.1.4 Flowability of binder, mortar, and concrete 20*
  - *3.1.5 Shrinkage 23*
  - *3.1.6 Durability (chloride and sulfate resistance) 23*
  - *3.1.7 Flexural strength 24*
  - *3.1.8 Compressive strength 25*
- 3.2 Structural test results for rehabilitated ties 26
  - *3.2.1 Tie preparation 26*
  - *3.2.2 Flexural tests 27*
  - *3.2.3 Compressive strength test 37*
- 3.3 Lessons learned 38

4 Economic Analysis 39

4.1 Costs and assumptions 39
4.1.1 Alternative 1 (commercially available crossties) 40
4.1.2 Alternative 2 (demonstrated technology) 40
4.2 Projected return on investment (ROI) 41

5 Conclusions and Recommendations 43
5.1 Conclusions 43
5.2 Recommendations 43
5.2.1 Applicability 43
5.2.2 Implementation 44
5.2.3 Future work 44

References 45

Report Documentation Page

Figures and Tables

Figures

Figure 1. Cross section of typical railroad track and foundations. 7
Figure 2. Tie plates. 8
Figure 3. AREMA failure modes that are treatable using in-place inorganic polymer application. 9
Figure 4. Railroad track is highlighted on aerial views at several candidate Army installations. (Source: Google Earth with overlays by ERDC-CERL. 10
Figure 5. Proctor test apparatus. 13
Figure 6. New, undamaged tie (left) and aged tie without rehabilitation (right) were tested as baselines. 13
Figure 7. Penetration test of Mix A. 17
Figure 8. Penetration test of Mix B. 17
Figure 9. Penetration test of Mix C. 18
Figure 10. Binder microstructure of (a) Mix A at 3 days; (b) Mix A at 28 days; (c) Mix B at 3 days; (d) Mix B at 28 days; (e) Mix C at 3 days; and (f) Mix C at 28 days. 19
Figure 11. (a) Microstructure of Mix 50 RT cured at 28 days, (b) unreacted slag at the center of the microstructure, (c) reacted portion showing cauliflower-shaped geopolymer precipitates, (d) unreacted angular particle identified as slag, and (e) plot of EDS data showing presence of Ca. 20
Figure 12. Various mixes shown during flowability observations. (a) Mix B binder; (b) Mix B with 40 wt% sand mortar; (c) Mix B with 20 wt% sand and 2.5 wt% basalt concrete; (d) Mix A binder (e) Mix A with 25 wt% sand mortar; and (e) Mix A with 15 wt% sand and 2.5 wt% basalt concrete. 21
Figure 13. Nesting of fibers observed due to incomplete mixing. 22
Figure 14. Damaged railroad ties before rehabilitation (continued to next page). 26
Figure 15. Undamaged tie under vertical load. 27
Figure 16. Rehabilitated tie #1, before flexural testing. 28
Figure 17. Rehabilitated tie #1 after flexural loading. 28
Figure 18. Cross section of post-tested tie #1–5 showing good penetration of inorganic polymer into wood. 29
Figure 19. Rehabilitated tie #2 before flexural testing. 29
Figure 20. Rehabilitated tie #2 after flexural testing. 30
Figure 21. Rehabilitated tie #5 before testing 30
Figure 22. Rehabilitated tie #5 after vertical load testing. 31
Figure 23. Load-deflection of specimen #1. 31
Figure 24. Load-deflection of specimen #2. 32
Figure 25. Load-deflection of specimen #3. 32
Figure 26. Load-deflection of specimen #4. 33
Figure 27. Load-deflection of specimen #5. 33

Figure 28. Load vs deflection curves of rehabilitated ties #1–5. 34
Figure 29. Load vs deflection curves of new and aged undamaged railroad ties. 34
Figure 30. Stress vs deflection curves of rehabilitated ties #1–5. 35
Figure 31. Stress vs deflection curves of damaged and undamaged railroad ties (only wood, no binder). 36

Tables

Table 1. Mass and mass fractions of Mixture A components. 14
Table 2. Mass and mass fractions of Mixture B components. 15
Table 3. Mass and mass fractions of Mixture C components. 15
Table 4. Shrinkage of concrete mixes A, B, and C. 23
Table 5. Chloride and sulfate resistance of Mix A, Mix B, and Mix C concretes. 24
Table 6. Stress and strain during curing time. 25
Table 7. Material composition and compressive strength of developed mixtures. 25
Table 8. Consolidated test data of rehabilitated railroad ties. 36
Table 9. Rehabilitated railroad ties specifications. 37
Table 10. Mass percent of mix components. 37
Table 11. Cube test results. 38
Table 12. Approximate cost of each binder mixture. 39
Table 13. ROI calculation (values in thousands of dollars). 42

Unit Conversion Factors

Multiply	By	To Obtain
cubic feet	0.02831685	cubic meters
feet	0.3048	meters
inches	0.0254	meters
pounds (mass)	0.45359237	kilograms
pounds (mass) per square inch	6894.75729	pascals
square inches	6.4516 E-04	square meters

Preface

This study was conducted for the Office of the Secretary of Defense (OSD) under Corrosion Prevention and Control (CPC) Program Project F17-AR03, "Rehabilitation of Deteriorated Wood Railroad Ties Using Inorganic Polymers." The proponent was the U.S. Army Office of the Assistant Chief of Staff for Installation Management (ACSIM), and the stakeholder was the U.S. Army Installation Management Command (IMCOM). The technical monitors were Robert A. Herron (OUSD(A&S), Materiel Readiness, Corrosion Policy and Oversight), Ismael Melendez (IMPW-E), and Valerie D. Hines (DAIM-ODF).

The work was performed by the Materials and Structures Branch of the Facilities Division (CEERD-CFM), U.S. Army Engineer Research and Development Center, Construction Engineering Research Laboratory (ERDC-CERL). Dr. Ghassan K. Al-Chaar (CEERD-CFM) was the Principal Investigator. A portion of this work was supervised by Dr. Waltraud M. Kriven, Department of Materials Science and Engineering, University of Illinois at Urbana-Champaign. At the time of publication, Vicki L. Van Blaricum was Chief, CEERD-CFM; Donald K. Hicks was Chief, CEERD-CF; and Michael K. McInerney, CEERD-CFM, was the ERDC CPC Program Coordinator. The Deputy Director of ERDC-CERL was Dr. Kirankumar Topudurti, and the Director was Dr. Lance D. Hansen.

Marion L .Banko is gratefully acknowledged for her work and persistence in verifying data compiled during the laboratory testing phase of this project.

The Commander of ERDC was COL Ivan P. Beckman, and the Director was Dr. David W. Pittman.

1 Introduction

1.1 Problem statement

The U.S. Army owns and operates roughly 1,900 miles of railroad track. The majority of this track uses creosote-treated wood crossties to support the rails. When wood ties deteriorate to the point they can no longer support the specified load, they must be removed and replaced. The Army replaces several thousand wood ties annually due to deterioration. When a deteriorated tie is not replaced promptly, its load must be carried by the rails and adjacent ties. Deferral of tie replacement accelerates the degradation of these other components, which will reduce the planned service life of the track and often will make it necessary to reduce train speeds to maintain safety. Delays or rerouting may even become necessary if emergency repairs become necessary.

When deteriorated wood ties are removed from the track, the creosote-treated waste becomes a disposal problem for the Army. National and state environmental regulations have become significantly more restrictive over several decades, and landfill disposal of commercial quantities of creosote-treated wood is essentially prohibited nationwide. Even the sale of the used ties for consumer uses has been mostly discontinued due to potential legal liability. For similar reasons, the use of waste railroad ties for energy cogeneration has also greatly declined. Any reduction in the use and disposal of creosote-treated wood ties would benefit Army railroad operational efficiency and reduce potential Army exposure related to environmental disposal regulations.

Engineered thermoplastic composite crossties have been introduced to the market as an improvement over wood ties. When fabricated using post-consumer recycled plastics, they can provide an environmental benefit while avoiding the costs and problems of hazardous waste disposal. They are commercially available in quantity and provide longer service life than treated wood ties. However, these thermoplastic products typically cost more than double per unit compared to conventional wood ties ($180 per plastic tie versus $75 per wood tie in 2017 dollars). Consequently, the high first cost of procuring thermoplastic composite crossties likely makes them unaffordable for large-scale use by the Army.

A cost-effective alternative technology could make it possible to rehabilitate timber crossties in place, a rehabilitation method that would reduce procurement costs, reduce disposal costs, and avoid significant railroad traffic interruptions during repair activities. Specifically, the capability of rejuvenating an existing deteriorated wood tie to extend its design life by another 30–50 years would greatly reduce crosstie life-cycle costs while also reducing the Army's burden of disposing creosote-treated ties.

Geopolymers have been used to repair wood structural members (Ferdous et al. 2015), but they have not yet been demonstrated and validated for the repair and rehabilitation of heavily degraded wood railroad crossties. Inorganic polymer blends that contain geopolymers and other components such as slag fly ash binders (Al-Chaar et al. 2017) constitute a promising family of materials that might be synthesized into a cementitious paste that is then optimized to fill splits and voids in decomposed wood railroad ties. Such materials could potentially meet all of the railroad maintenance and repair requirements stated above and provide a simpler and more environmentally benign solution to the replacement and disposal of creosote-treated wood ties.

A focused development, testing, and validation project sponsored under the Department of Defense Corrosion Prevention and Control (CPC) Program was executed by the U.S. Army Engineer Research and Development Center, Construction Engineering Research Laboratory (ERDC-CERL) and the Materials Science and Engineering Department at the University of Illinois at Urbana-Champaign.

1.2 Objectives

The objectives of this work were to develop, optimize, and test several prototypes of cementitious inorganic polymer blends that would prove suitable for in situ rehabilitation of deteriorated creosote-treated wood crossties within operational Army railroad lines.

1.3 Approach

The raw materials used in this study were chosen on the basis of availability, chemical composition, and cost. All work on this project was directly informed by the standards for railroad track established by the American

Railway Engineering and Maintenance-of-Way Association (AREMA).* All material and specimen testing was performed in accordance with the industry standards cited throughout the main text. Details of the testing and validation work are described in Chapter 2.

1.4 Metrics

Listed below are the performance metrics for critical properties of the geopolymer repair material alongside the industry standard or test method used to evaluate each candidate mixture:

- Compressive strength greater than 5,000 psi (ASTM C1424)
- Good flexural strength (ASTM C78)
- Optimal flowability
- Reasonable set time (ASTM C191 – Vicat; ASTM C403 – Proctor)
- Minimal shrinkage and excellent bonding (ASTM C157)
- High resistance to chlorides and sulfates (ASTM C267)

The *AREMA Design Manual* (Vol 1; Ch 4, 5, and 30) was the source of guidance and criteria for selecting the damaged tie specimens used in the rehabilitation testing.

The following characteristics of molded, cured geopolymer specimens used in crosstie rehabilitation were then tested to validate whether those materials met industry performance metrics for critical railway performance parameters:

- Bending strength and stiffness (ASTM C293 [crosstie flexure/bending] and ASTM C78 [flexure of molded and cured geopolymer blends])
- Rail seat compressive strength and rebound† (ASTM C1424 [compression of molded and cured geopolymer blends])
- Spike hold
- Impact resistance relative to handling
- Wheel derailment
- Effects of aging on treated tie properties

* Lanham, MD. www.arema.org

† This item and the four that follow it were established for the in situ field tests, but that work could not be coordinated in time to be completed during the project schedule. See section 1.5 for more.

1.5 Scope of execution

As originally proposed, the project was to include in situ field validation tests of the most promising candidate geopolymer blends on a section of operational railroad track at Fort Campbell, Kentucky. However, it was discovered that preparing such a demonstration would involve unexpected, time-consuming coordination with railroad operators for such purposes as identifying candidate ties, ensuring safe railroad operations, and minimizing freight traffic interruptions. This extensive coordination put the timeline of in situ field validation outside this project's duration. Consequently, this project's scope was limited to evaluating the properties of three candidate repair materials and rigorous laboratory testing to ascertain the materials' suitability for field application.

See section 5.2.3 for a brief description of follow-on work proposed to collect sufficient in situ field data to validate the technology for DoD implementation.

2 Technical Investigation

2.1 Technology overview

Geopolymers are a class of amorphous, refractory, inorganic polymers that can be processed as a fluid and cured at room temperature (Davidovits 1982). They are typically synthesized by mixing amorphous aluminosilicate powders (e.g., metakaolin, fly ash, or slag) with an alkali silicate solution (Davidovits 1991; Davidovits et al. 2014). The formation of geopolymers can be summarized as (1) the dissolution of the aluminosilicate source in the alkali silicate solution, (2) polycondensation, and (3) precipitation (Kriven 2010; Ribero and Kriven 2016).

The term geopolymer is well established. Inorganic polymers are a closely related category of materials; they are not actual geopolymers, but they may incorporate up to 10% geopolymer content. Slag and fly ash binders (SFBs) have been well documented in previous literature (Rostami and Silverstrim 1996; Sindhunata et al. 2006; Davidovits, Davidovits, and Davidovits 2012). SFBs, which are a common component of inorganic polymers, have been made by mixing fly ash and/or slag with alkali silicate solution or by mixing alkali hydroxide and alkali silicate solution. There are several scientific papers that discuss the production of binders using slag, fly ash, alkali silicates and/or alkali hydroxides, alkali carbonates, and sulfates (Duxson et al. 2007; Puligilla and Mondal 2013; Bernal et al. 2013). However, SFBs are also made by mixing alkali silicates with certain aluminosilicate(s) like slag, class F fly ash, and metakaolin. It should be noted that different names have been given to these binders in the literature, but all can be broadly categorized as SFBs.

Stated in less-technical language, SFBs use inexpensive industrial byproducts as precursors—namely, slag and fly ash. The precursors are mixed with an alkali silicate solution to produce an SFB. When the binder is properly designed, it can have reasonable setting time and excellent compressive strength when compared to ordinary Portland cement (OPC). If the precursors are sourced properly, their use can lead to up to 90% reduction in carbon emissions through using recycled precursors and avoiding the use of OPC, the manufacturing of which emits carbon dioxide. (Davidovits 2013). Various particulate and fibrous filler phases can be added to SFBs to increase tensile strength, to reduce shrinkage and cracking, and to make useful engineering materials (Rill, Lowry, and Kriven 2010; Musil,

Kutyla, and Kriven 2012; Musil and Kriven 2014; Ribero and Kriven 2016; Sankar et al. 2017). The two binding phases that are present in SFBs are (1) calcium silicate hydrate with various degrees of aluminum substitution (denoted as C(A)SH) and (2) geopolymers (Yip, Lukey, and Van Deventer 2005).

Davidovits, Davidovits, and Davidovits (2012) developed user-friendly slag-fly ash geopolymer mixtures using class F fly ash, ground granulated blast furnace slag, and alkali silicate (molar silicon dioxide [SiO_2]: sodium dioxide [Na_2O]) with a strength modulus from 1.25 to 1.85. However, the amount of slag did not increase beyond 18% by weight, and the amount of fly ash varied 58%–63% by weight. The rheology of the binder and the design of mortar and concrete mixtures using this binder were not discussed.

For the work discussed here, new SFB mixtures were created by ERDC-CERL researchers. It was found that the developed mixtures were easy to prepare onsite, were cost effective, had excellent flow, and had excellent compressive and flexural strengths. In order to validate these mixtures for use in crosstie rehabilitation, they were prepared and poured into voids within deteriorated wooden ties. Flexural tests were performed on the rehabilitated railroad ties and compared with flexural tests on damaged ties and undamaged ties.

2.2 AREMA track design standards

AREMA track design standards heavily influence the properties required of the SFB application for rehabilitating crossties. The SFB material must, for example, perform safely and effectively in terms of rail hardware fastening requirements and varieties of stress imposed by train traffic and environmental conditions. Understanding some detail of track design standards provides insight into the performance requirements for the SFB application.

The industry source of standards and procedures for railroad design and rehabilitation is the AREMA design manual, *Manual for Railway Engineering* (MRE),* an annual publication released each April. An automated design-support computer application called TRACK is available to facilitate AREMA-compliant designs. A considerable disadvantage of manual design, however, is that little data are available to correlate the value of

* Specifically Volume 1, Chapter 4 “Rail,” Chapter 5 “Track,” and Chapter 30 “Ties.”

track modulus with the properties of individual track components such as the crossties. Railroad track carrying annual traffic volumes of 5 MGT (million gross tons) or lower is common at military installations. In such a use case, wood ties are more likely to fail from decay than from either mechanical wear or loss of spike-holding capability. The two common cross-sectional sizes for wood crossties are (1) 7 in. thick x 9 in. wide and (2) 6 in. thick x 8 in. wide. The 7 x 9 in. ties are recommended for areas with higher traffic volumes and wheel loads, as well as for use in turnouts and road crossings. Track ties are commonly produced in 8.5 ft or 9 ft lengths, and the 8.5 ft length is used for standard ties when most conveniently available. The typical cross section of track is shown in Figure 1.

Figure 1. Cross section of typical railroad track and foundations.

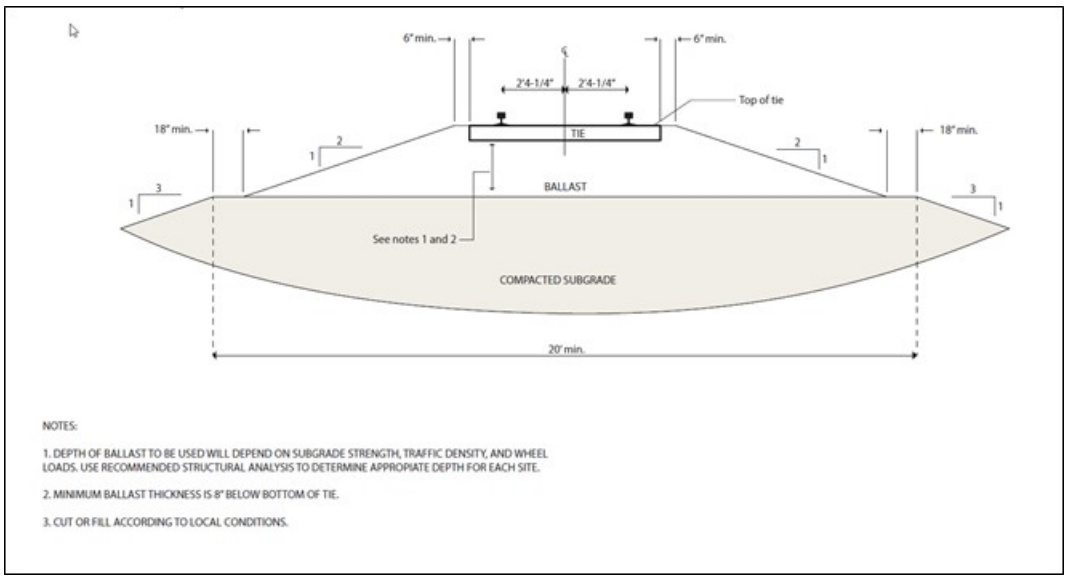

Another critical component of railroad track—tie plates—also varies in available length and width. Most sizes are suitable as long as the spike hole punching (or distance between the shoulders for double-shoulder plates) matches the width of the rail base. Either single- or double-shoulder tie plates can be used (see Figure 2). For double-shoulder tie plates, the distance between the shoulders will be at most 1/8 in. larger than the rail base width. On single-shoulder plates, the spike holes on the gage side (opposite the shoulder) must keep the inside face of the spike within 1/8 in. of the rail base when the opposite edge of the base is against the shoulder. Within a given length of track, tie plates of different lengths and widths may be used, and single-shoulder plates may be mixed with double-shoulder plates. However, plates with different cants (i.e., those with level rail

seats and those with a 1:40 slope) will not be mixed. Tie plates with a 1:40 cant are preferred.

On tangent (i.e., straight) track and on curves up to 4 degrees, one spike on the gauge side and one spike on the field side of each rail will be used (a total of four spikes in each tie). On curves greater than 4 degrees, one spike on the field side and two spikes on the gauge side of each rail will be used (a total of six spikes in each tie).

Figure 2. Tie plates.

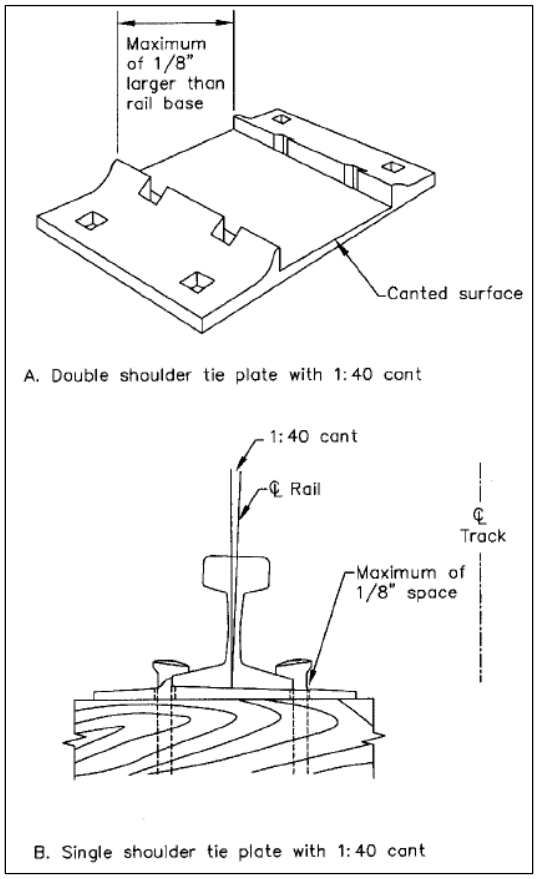

AREMA standards consider a wood tie to be defective if it is

- broken through
- split or otherwise impaired to the extent that it will not hold spikes or other rail fasteners
- so deteriorated that the tie plate can move more than 0.5 in. laterally relative to the crosstie
- cut more than 2 in. by the tie plate

- cut by wheel flanges, dragging equipment, fire, etc., to a depth of more than 2 in. that is within 12 in. of the base of the rail, frog, or load-bearing area
- rotted, hollow, or generally deteriorated to a point where a substantial amount of the material is decayed or missing
- end-broken, including specimens in which the defect extends beneath the base plate and is not noticeable except for a small rise in the end of the tie from the plane at the center portion.

Modes of failure that could be reversed by using inorganic polymer repair-in-place techniques are shown in Figure 3.

Figure 3. AREMA failure modes that are treatable using in-place inorganic polymer application.

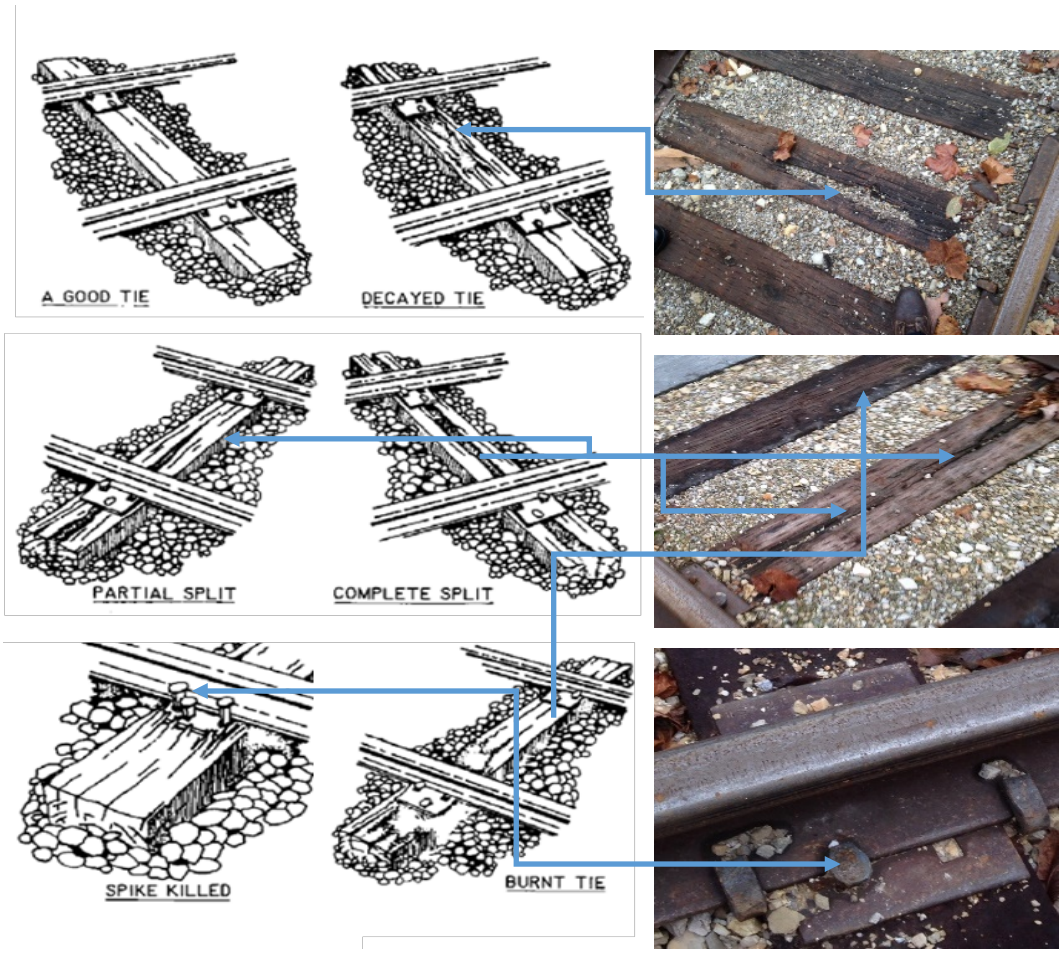

2.3 Candidate field test sites

According to an environmental assessment of the railroad at Fort Campbell from 2006, there are approximately 17 miles of railroad track connected to a rail spur located south of Gate 2. In addition, Figure 4 shows aerial views of tracks at three other Army installations under consideration as locations to apply the candidate technology.

Figure 4. Railroad track is highlighted on aerial views at several candidate Army installations. (Source: Google Earth with overlays by ERDC-CERL.

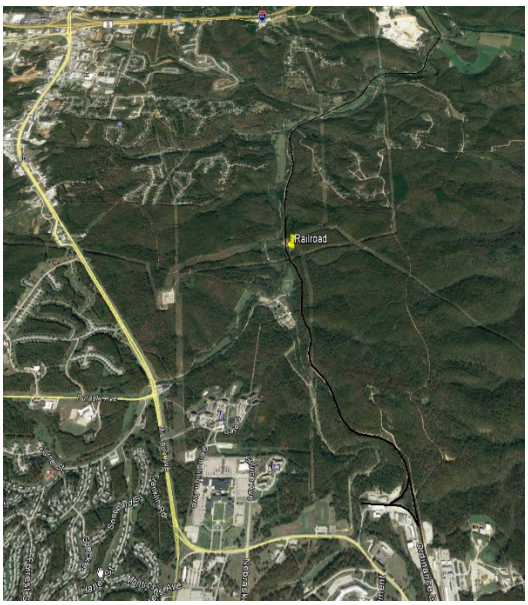

Fort Leonard Wood

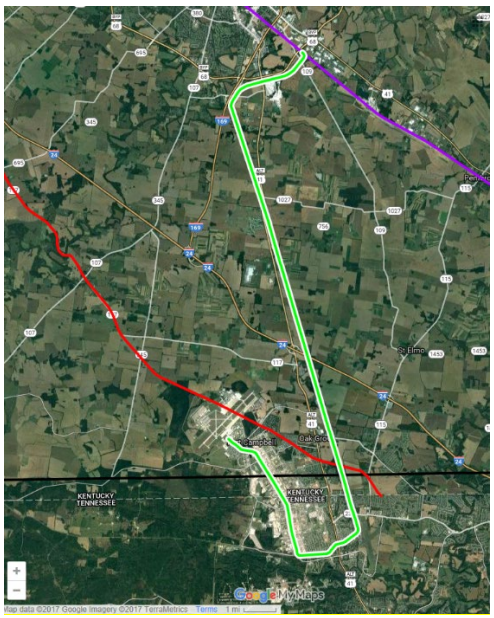

Fort Campbell

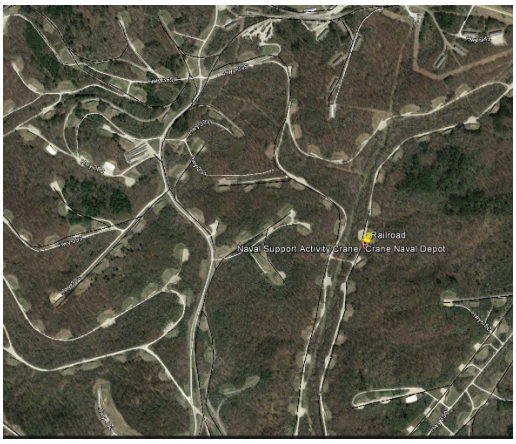

Crane Naval Depot

McAlester Army Ammunition Plant

Until 1981, the Illinois Central Gulf (ICG) Railroad System provided rail service to Fort Campbell. After 1981, the Army purchased the rail lines and the right-of-way in order to continue rail service on the installation. More

rail and property have recently been purchased to allow Fort Campbell to connect with the CSX* main rail line near Hopkinsville, Kentucky.

2.4 Inorganic polymer tests

2.4.1 Compression

Mortar and concrete were formed into a 2-inch cube specimen. The cubes were cast on polyethylene molds with petroleum jelly as the mold release. Binders were 1 in. diameter and 2 in. high, and they were cast on polyoxymethylene (Delrin™) molds coated inside with petroleum jelly as the mold-release agent. The molds with specimens were covered with a wet towel and wrapped in a plastic food-service film to prevent escape of water and potential cracking. They were tested using a compression machine located at ERDC-CERL. Samples were tested in accordance with ASTM C403 (2006) and ASTM C1424 (2010) standards.

2.4.2 Flexure

Concrete samples were cast in 3 x 3 x 12 in. steel molds with petroleum jelly as the mold release. Samples were tested using a four-point bend testing configuration specified in ASTM C78 (2016).

2.4.3 Shrinkage

Concrete samples were cast on a mold that conforms to the ASTM C157 (2014) standard with some modifications. The mold dimensions were 1 x 1 x 11.25 in. The modification is that mixes A, B, and C concrete samples were cured in a plastic zip-seal bag with a wet towel in it for 7 days. Shrinkage for each of the samples was measured using a calibrated comparator at 4, 7, 14, and 28 days.

2.4.4 Durability

Binder cylinders of 1 in. diameter and 2 in. height, and 2 in. concrete cubes were tested for chloride and sulfate resistance. These specimens were immersed in sulfuric acid and hydrochloric acid for 7, 14, and 28 days, according to two standards, ASTM C267 (2015) and ASTM C1012 (2015), with some modifications. Following Zubrod (2013), specimens were submerged in 15% solution of sulfuric and hydrochloric acids. Mass loss was

* CSX was established in 1980 as part of the Chessie System and Seaboard Cost Line Industries merger.

measured after 7, 14, and 28 days of submersion, and the specimens were tested in compressive strength according to ASTM C1424 (2015).

2.4.5 Setting time

Setting is defined as the transition of a material from a fluid to solid phase, before it gains compressive strength. Penetration-resistance testing is the standard for quantifying the setting time of cementitious materials (Suraneni et al. 2014). The testing device measures mechanical resistance to penetration of cement pastes or mortars by needles over time. There are primarily two penetration resistance tests done on cementitious materials: (1) ASTM C191, the Vicat test; (2) and ASTM C403, the Proctor penetration-resistance test. The Vicat test uses only one needle for penetration and is typically used for very stiff cement pastes having dough-like consistency due to low water content (Chung et al. 2017). The Vicat test does not provide information on the evolution of stiffening with time. Instead, setting times are estimated by measuring the penetration depth of a single needle while maintaining a constant load. In contrast, the Proctor test measures the resistance offered by the medium against a penetrating needle (initially developed for cement mortar extracted from concrete but later extended to cement; Chung et al. 2017). Cement mortar does not provide any resistance to penetration immediately following the mixing. As hydration continues and the microstructure develops, resistance to the penetrating needle increases. This resistance measurement helps in monitoring the rate of hardening/strength gain. According to the standard, the initial setting of OPC-based concrete occurs when the extracted mortar shows a penetration resistance of 3.5 MPa, and the final set occurs at a penetration resistance of 27.3 MPa. It should be noted that this value range is arbitrary, and no further chemical changes occur in the concrete upon setting (Chung et al. 2017).

Setting time of binders was measured using ASTM C403 Proctor penetration resistance test. This test was originally developed for mortars sieved from concrete. Penetration tests measure gel strength. Based on previous studies that extended ASTM C403 to cements, initial set was empirically assigned when penetration resistance reached 2 MPa, and final set was assigned when penetration resistance reached 14 MPa. See Figure 5 for proctor test apparatus.

Figure 5. Proctor test apparatus.

2.5 Structural testing of repaired ties

Damaged crossties were selected for rehabilitation using candidate inorganic polymer mixes. Structural strength of the rehabilitated ties was tested in accordance with ASTM C293. Figure 6 shows the three-point test setup with an undamaged crosstie (left) and a non-rehabilitated specimen taken from field service (right) mounted in the testing device.

Figure 6. New, undamaged tie (left) and aged tie without rehabilitation (right) were tested as baselines.

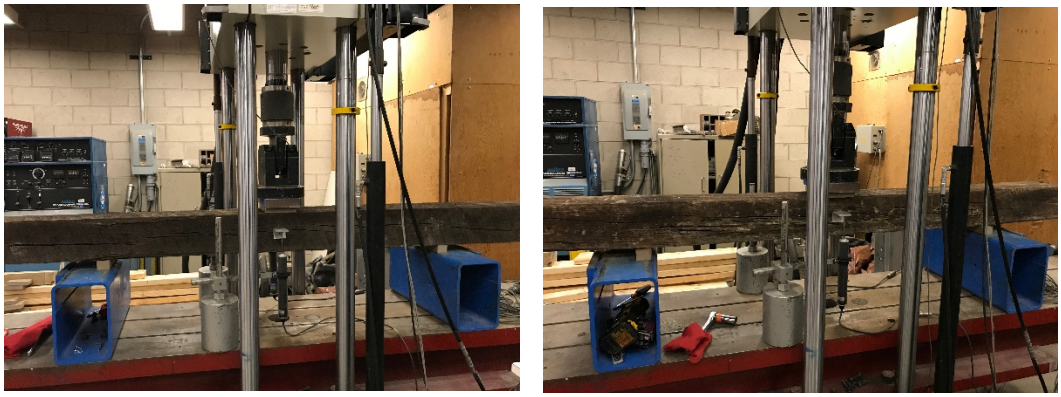

3 Results

3.1 Binder, mortar, and concrete results

3.1.1 Material nomenclature and compositions

Table 1, Table 2, and Table 3 show the compositions of the three candidate geopolymer blends used in this project. In the tables, these are designated Mix A, B, and C, respectively. Each table has three compound rows, one each identifying composition of the binder, the mortar, and the geopolymer concrete. These rows include the binder composition, and the mass and mass fraction of components added to create the binder and the patch of geopolymer concrete. Note that the concrete consists of the mortar plus chopped basalt fiber.

Table 1. Mass and mass fractions of Mixture A components.

Mixture	Component Name	Component Mass (kg)	Mass Fraction (%)
Mix A Binder	Metso 2048	0.52	10.00
	Water	1.49	29.00
	Class F Fly Ash	1.29	25.00
	Grade 120 Slag	1.08	21.00
	Metastar 501 MK	0.77	15.00
	CERL Sand	0.00	0.00
	Basalt 1/2 in.	0.00	0.00
Mix A Mortar	Metso 2048	5.98	7.50
	Water	17.34	21.75
	Class F Fly Ash	14.95	18.75
	Grade 120 Slag	12.56	15.75
	Metastar 501 MK	8.97	11.25
	CERL Sand	19.93	25.00
	Basalt 1/2 in.	0.00	0.00
Mix A Concrete	Metso 2048	9.52	8.21
	Water	27.60	23.79
	Class F Fly Ash	23.80	20.51
	Grade 120 Slag	19.99	17.23
	Metastar 501 MK	14.28	12.31
	CERL Sand	17.85	15.38
	Basalt 1/2 in.	2.98	2.56

Table 2. Mass and mass fractions of Mixture B components.

Mixture	Component Name	Component Mass (kg)	Mass Fraction (%)
Mix B Binder	Metso 2048	3.73	10.00
	Water	9.33	25.00
	Class F Fly Ash	12.13	32.50
	Grade 120 Slag	12.13	32.50
	Metastar 501 MK	0.00	0.00
	CERL Sand	0.00	0.00
	Basalt 1/2 in.	0.00	0.00
Mix B Mortar	Metso 2048	4.70	6.00
	Water	11.75	15.00
	Class F Fly Ash	15.27	19.50
	Grade 120 Slag	15.27	19.50
	Metastar 501 MK	0.00	0.00
	CERL Sand	31.32	40.00
	Basalt 1/2 in.	0.00	0.00
Mix B Concrete	Metso 2048	11.02	7.69
	Water	27.55	19.23
	Class F Fly Ash	35.82	25.00
	Grade 120 Slag	35.82	25.00
	Metastar 501 MK	0.00	0.00
	CERL Sand	29.39	20.51
	Basalt 1/2 in.	3.67	2.56

Table 3. Mass and mass fractions of Mixture C components.

Mixture	Component Name	Component Mass (kg)	Mass Fraction (%)
Mix C Binder	Metso 2048	1.24	5.53
	Water	6.87	30.75
	Class F Fly Ash	2.97	13.27
	Grade 120 Slag	5.34	23.89
	Metastar 501 MK	5.93	26.55
	CERL Sand	0.00	0.00
	Basalt 1/2 in.	0.00	0.00
Mix C Mortar	Metso 2048	0.99	4.15
	Water	5.49	23.06
	Class F Fly Ash	2.37	9.95
	Grade 120 Slag	4.27	17.92
	Metastar 501 MK	4.74	19.91

Mixture	Component Name	Component Mass (kg)	Mass Fraction (%)
	CERL Sand	5.95	25.00
	Basalt 1/2 in.	0.00	0.00
Mix C Concrete	Metso 2048	0.99	4.56
	Water	5.52	25.35
	Class F Fly Ash	2.38	10.94
	Grade 120 Slag	4.29	19.70
	Metastar 501 MK	4.77	21.89
	CERL Sand	3.28	15.05
	Basalt 1/2 in.	0.55	2.51

3.1.2 Setting time

The penetration testing method for setting is well understood, simple, inexpensive, and easy to use. However, it is also labor intensive, time consuming, and does not provide continuous data output. Because the purpose of ASTM C403 is to measure time of setting of mortar extracted from concrete, the values of penetration resistance in paste correspond to initial and final set in concrete. These values are 2 MPa for initial set and 14 MPa for final set (Chung et al. 2017; Kriven, Bell, and Gordon 2003.).

Penetration tests provide a better idea of how stiff the binder gets with time. Figure 7 plots penetration test results on Mix A, with initial set at 95 minutes and final set at 280 minutes. As shown in Figure 8, Mix B set at 125 minutes and achieved final set at 233 minutes. Figure 9, for Mix C, shows initial set at 60 minutes and final set at 270 minutes.

Figure 7. Penetration test of Mix A.

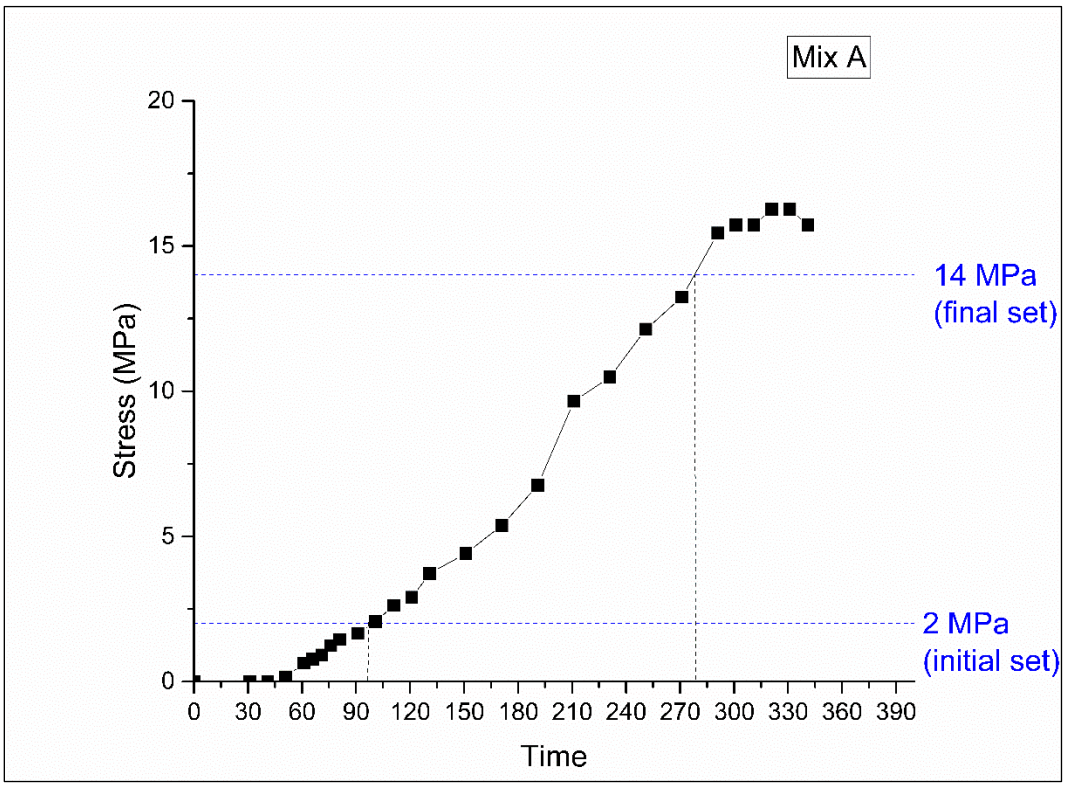

Figure 8. Penetration test of Mix B.

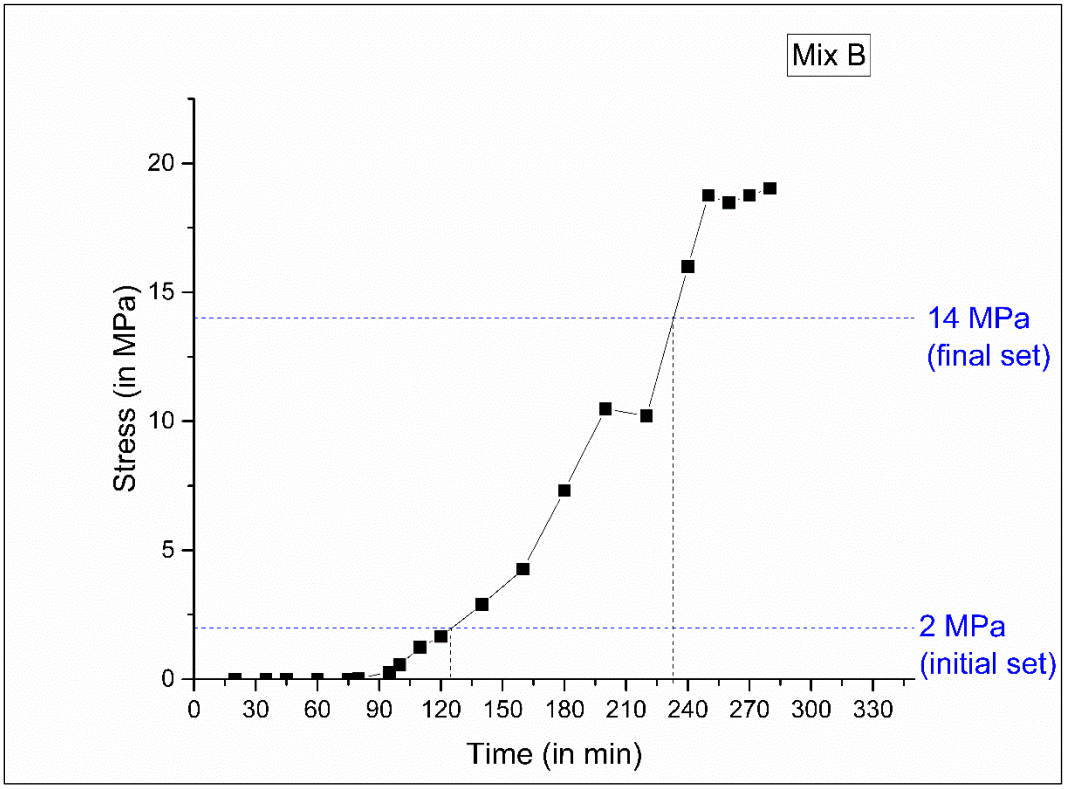

Figure 9. Penetration test of Mix C.

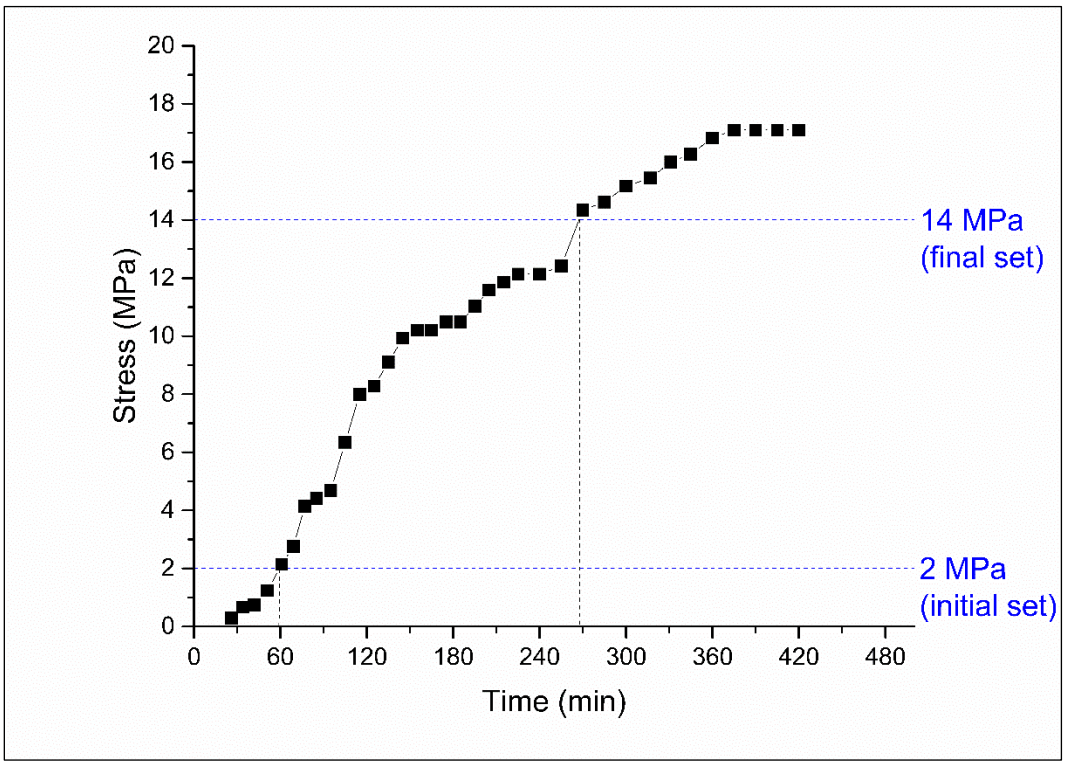

3.1.3 Microstructural analysis

This testing program was executed at ERDC-CERL and the University of Illinois Materials Research Laboratory. Photographic data produced through an energy-dispersive spectrometry (EDS) microstructural analysis of three mixes are presented in Figure 10. Microstructure of Mix A at 3 days (Figure 10a) showed unreacted fly ash glassy cenospheres embedded in a matrix. The exact composition of this matrix is not known because the result was altered due to the unreacted fly ash. However, it is suspected to contain geopolymer as well as calcium silicate hydrates with a varying degree of aluminum (Al) substituting for silicon (denoted as C-(A)-S-H). The microstructure of Mix A at 28 days shows fly ash cenospheres in a more compact matrix (Figure 10b). The microstructure of Mix B at 3 days (Figure 10c) is similar to Mix A in that unreacted fly ash cenospheres are embedded in a matrix, but the microstructure seems to be more compact than Mix A at the same age (3 days). This added compaction may help to explain the comparative strength results for Mix B versus Mix A, discussed in section 3.1.8).

Figure 10. Binder microstructure of (a) Mix A at 3 days; (b) Mix A at 28 days; (c) Mix B at 3 days; (d) Mix B at 28 days; (e) Mix C at 3 days; and (f) Mix C at 28 days.

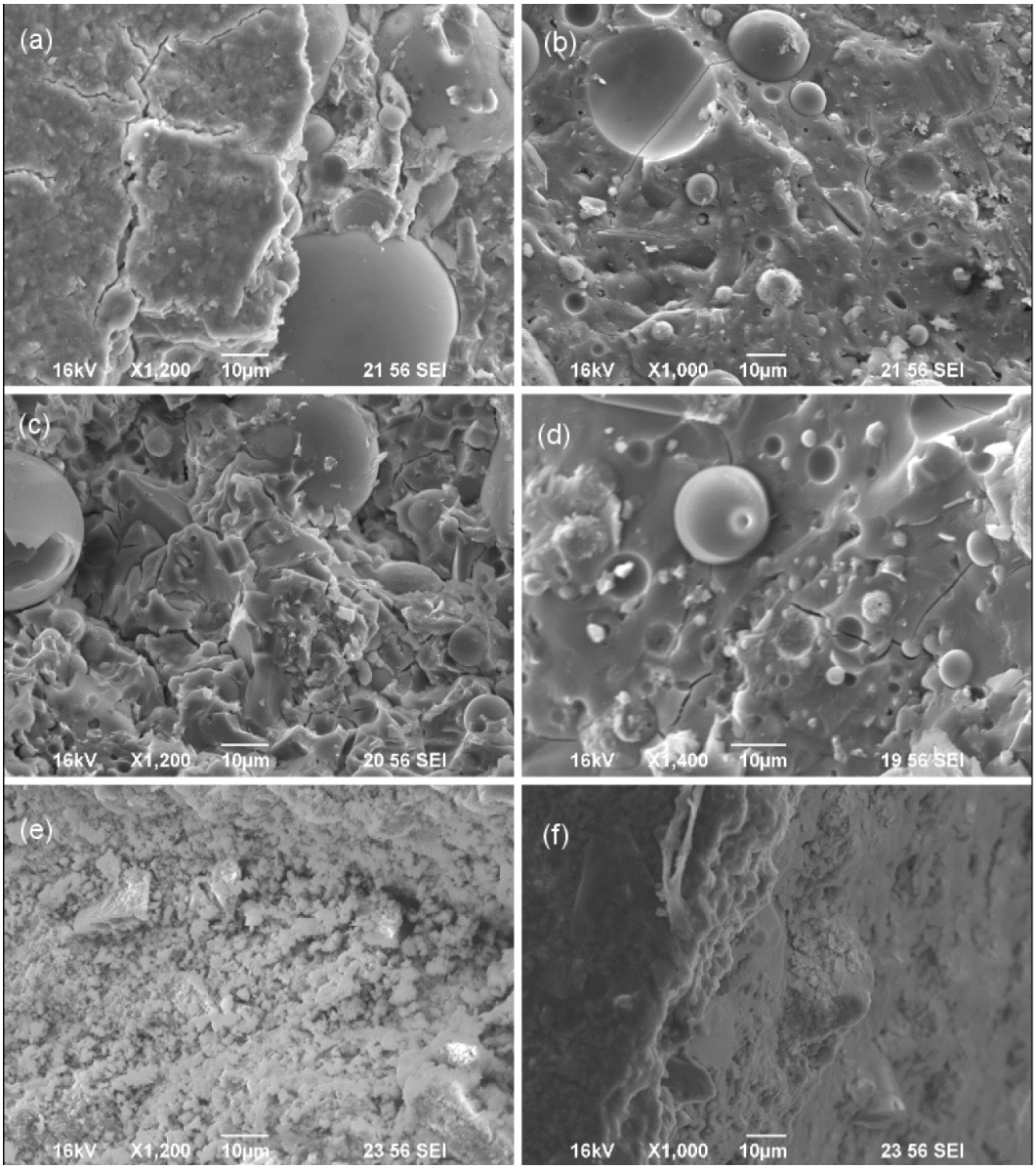

The microstructure of Mix B (Figure 10d) becomes more compact at 28 days. The microstructure of Mix C at 3 days shows some unreacted precursor (angular and platelet-like morphology) (Figure 10e) and some lumpy (cauliflower-like) precipitates (Figure 10f) that are generally observed in stoichiometric geopolymers. Microstructure becoming more compact with time correlates well with strength development over time.

Figure 11 shows the microstructure of Mix C (Figure 11a), unreacted slag (Figure 11b), the reacted portion showing cauliflower-shaped geopolymer precipitates (Figure 11c), and proof that the unreacted angular particle is

slag through use of energy-dispersive spectrometry (EDS), which detected the presence of calcium (Ca) (Figure 11d and 11e).

Figure 11. (a) Microstructure of Mix 50 RT cured at 28 days, (b) unreacted slag at the center of the microstructure, (c) reacted portion showing cauliflower-shaped geopolymer precipitates, (d) unreacted angular particle identified as slag, and (e) plot of EDS data showing presence of Ca.

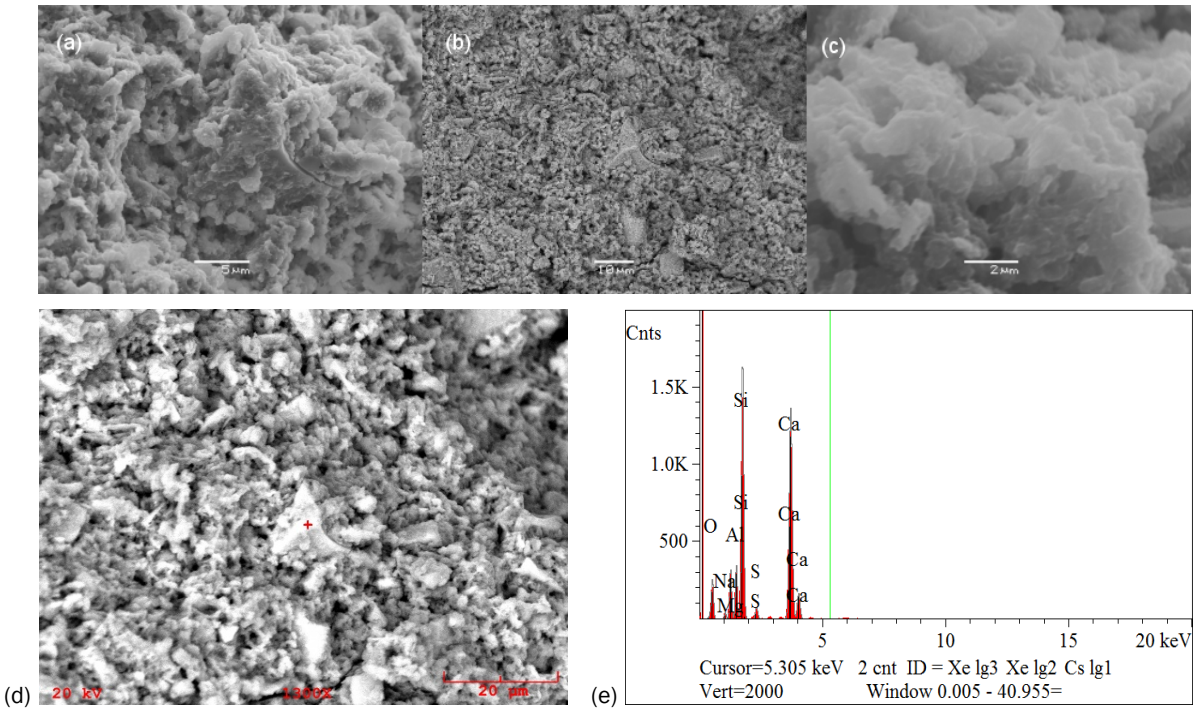

3.1.4 Flowability of binder, mortar, and concrete

This testing task was executed at the University of Illinois Materials Testing Laboratory. Well-graded fine sand was brought to saturated surface dry (SSD) condition and then added to Mix A and Mix 49 B mortars in increments of 5 weight percent (wt%), and its flowability was empirically observed as shown in Figure 12. Sand was preferable to chamotte because sand is less expensive and more readily available. Also, because chamotte needs high-temperature processing, using it increases the mixture's overall carbon footprint. It was found that up to 53 wt% well-graded fine sand in SSD could be added to Mix B mortar and up to 30 wt% well-graded fine sand in SSD could be added to Mix A mortar. If the amount of sand exceeded this amount, then no flow could be observed without vibration. Excellent flow without vibration resulted when the amount of sand is 40 wt% in Mix B mortar and 25 wt% in Mix A mortar. The mortar mixtures could flow into small cracks in the railroad tie.

Figure 12. Various mixes shown during flowability observations. (a) Mix B binder; (b) Mix B with 40 wt% sand mortar; (c) Mix B with 20 wt% sand and 2.5 wt% basalt concrete; (d) Mix A binder (e) Mix A with 25 wt% sand mortar; and (e) Mix A with 15 wt% sand and 2.5 wt% basalt concrete.

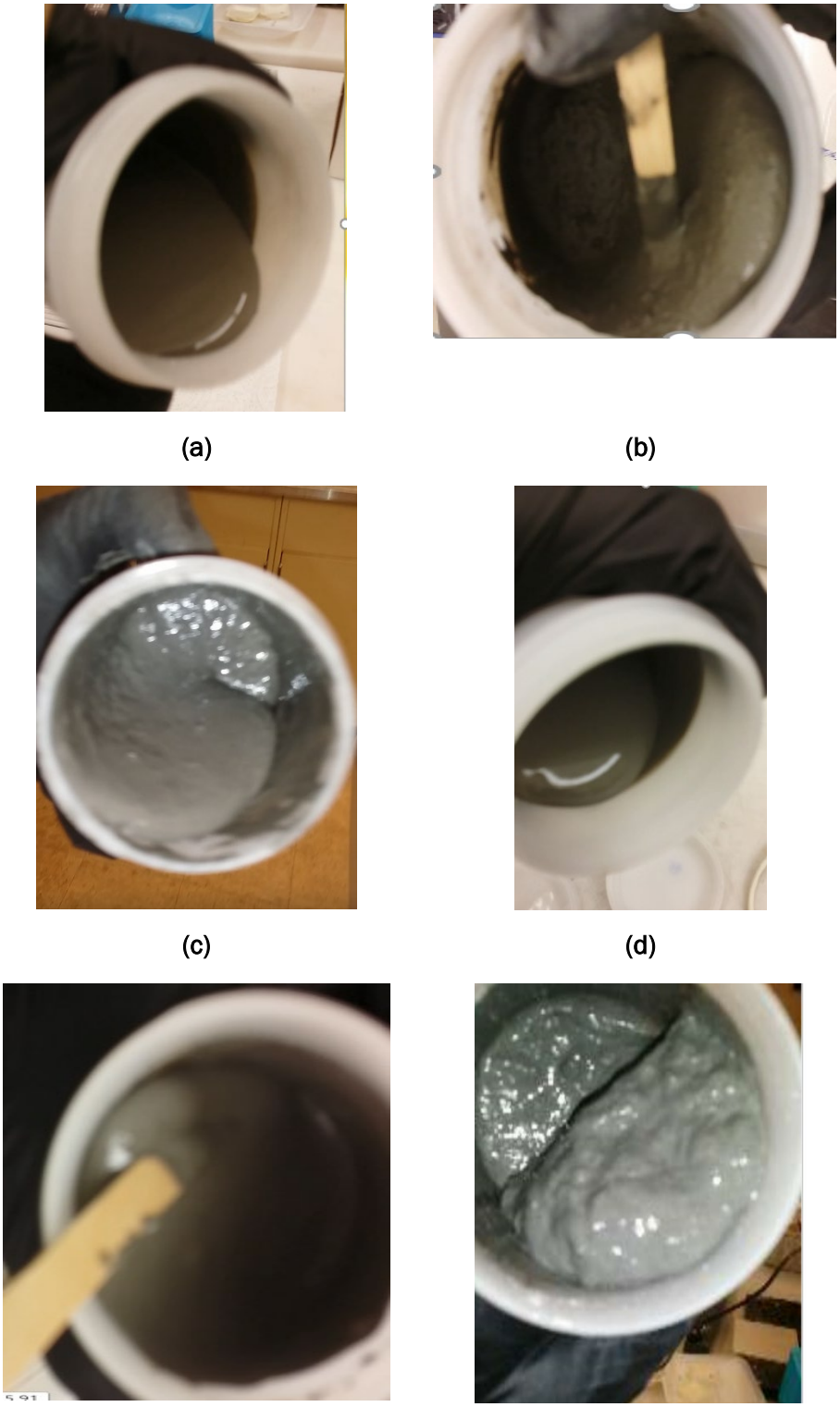

(a) (b)

(c) (d)

(e) (f)

Similar to sand, chopped basalt fibers of various length scales were used as reinforcements for Mix A and Mix B. In order to find out the optimum amount of basalt, the increments were 2.5 wt%. Chopped basalt fibers with sizing suitable for concrete applications was used from Sudaglass Fiber Technology.* It was found that 1-inch fibers were too long and resulted in loss of flow of binder due to the nesting of fibers. Nesting is defined here as entangling or clumping of fibers with matrix between them (Figure 13). One way to reduce nesting of fibers is to use the Thinky planetary mixer† which fluffs the fibers (breaks down a fiber tow) and randomly orients the basalt fibers to give the binder good flow. It was found that pre-fluffing of fibers can be done by using a shop vacuum, but adding pre-fluffed fibers to the binder still resulted in nesting. However, a similar effect to Thinky mixing was obtained by shear mixing the basalt fibers (without pre-fluffing) for an extended period of time (~15 minutes) and this lengthy shear mixing resulted in good flow.

Figure 13. Nesting of fibers observed due to incomplete mixing.

Finally, it was determined that 20 wt% sand and 2.5 wt% ½ in. basalt chopped unfluffed fibers was found to be ideal for Mix B. And 15 wt% sand and 2.5 wt% ½ in. basalt chopped unfluffed fibers were found to be ideal for Mix A (Figure 12). Such a mixture had good flow, graceful failure with enough warning, and avoided cracking from shrinkage when adequately sealed with a wet towel.

* Sudaglass Fiber Technology of Houston, Texas. www.sudaglass.com.

† Speedmixer™ by Thinky Corporation (FlackTeck, Inc., Landrum, SC, is U.S. distributor).

3.1.5 Shrinkage

Shrinkage testing performed on Mix A, B, and C concrete and are summarized in Table 4. It show that the drying shrinkage is very high when compared to OPC. Therefore, it is recommended that curing be done at 100% humidity conditions for 28 days.

Table 4. Shrinkage of concrete mixes A, B, and C.

Concrete Mix	4d length, change (%)	7d length, change (%)	14d length, change (%)	28d length, change (%)
A	2.011	1.959	1.953	1.951
B	2.410	2.408	2.401	2.400
C	2.205	2.140	2.099	2.022

3.1.6 Durability (chloride and sulfate resistance)

Preliminary durability tests were performed on binder Mixes A, B, and C binders, but the binders did not hold together. Hence a more practical choice of Mix A, B, and C concretes was adopted. Chloride and sulfate resistance of Mix A, B, and C concrete cubes of 2 inch dimensions were estimated by measuring the changes in mass, dimensions, and compressive strengths of cured control specimens and specimens submerged in acids for 7, 14 and 28 days. The acids were 15 wt% HCl and 15 wt% H2SO4. There was a mass loss with concretes submerged in hydrochloric acid and a mass gain with concretes submerged in sulfuric acid. The change in dimensions of the specimen seemed to be somewhat arbitrary. Minor or no loss in compressive strength was observed when time of submergence was low in HCl acid solution. However, the loss in compressive strength became significant when the time of submergence was high. In Mix A and Mix B concretes submerged in H_2So_4, there was an increase in compressive strength observed when compared to control samples at the same time of submergence which suggests curing continued during submergence (Table 5).

Table 5. Chloride and sulfate resistance of Mix A, Mix B, and Mix C concretes.

Mix	Submersion (Days)	Acid	Average Change				Compressive strength (psi)	
			Length (mm)	Width (mm)	Height (mm)	Mass (g)	Avg.	S.D.
A	7	Control	0.3	0.3	-0.2	-2.8	2205	318
	14	Control	0.3	0.3	-0.1	-2.3	2445	323
	28	Control	0.1	-0.1	-1.2	-9.6	24432	1566
	7	HCl	-2.7	-2.7	-1.8	-32.1	2396	356
	14	HCl	-1.6	-1.6	-0.6	-28.6	2017	269
	28	HCl	-1.9	-1.3	-0.8	-43.1	10593	993
	7	H2SO4	0.2	-0.1	-0.2	5.4	3004	1516
	14	H2SO4	0.3	0.3	0.1	1.7	3557	79
	28	H2SO4	0.6	0.0	-0.4	-2.1	12930	1243
B	7	Control	-0.1	0.4	0.2	-1.8	2762	452
	14	Control	0.3	0.3	-0.4	-3.6	3309	667
	28	Control	0.0	0.0	-0.8	-2.3	9723	1151
	7	HCl	-0.1	-0.1	0.1	-4.0	2614	481
	14	HCl	0.0	-0.3	-0.4	-13.3	2173	203
	28	HCl	1.0	0.0	1.0	-16.0	10993	1092
	7	H2SO4	0.6	0.6	0.5	2.7	3518	585
	14	H2SO4	0.2	0.2	0.0	1.6	4318	379
	28	H2SO4	1.6	0.8	-1.6	15.0	12357	3659
C	7	Control	0.0	0.0	-0.3	-1.6	1956	156
	14	Control	0.0	0.0	0.0	-16.9	16817	1625
	28	Control	0.0	-0.3	0.0	6.6	18170	229
	7	HCl	0.0	0.0	-0.7	-22.9	1477	340
	14	HCl	-2.7	-2.0	-0.7	-19.2	7630	1576
	28	HCl	-2.0	-2.0	-1.3	-56.2	7077	2455
	7	H2SO4	0.0	0.0	0.0	0.6	1684	172
	14	H2SO4	0.5	0.5	-0.3	-2.8	11553	867
	28	H2SO4	0.3	0.3	-0.3	1.3	9737	1735

3.1.7 Flexural strength

Flexural strength testing of Mix A, B, and C concretes was performed, and it was found that Mix A concrete had the highest flexural strength among the three. The flexural strength of Mix A and Mix C increased from 7 days to 14 days but decreased at 28 days. However, in Mix B, the flexural

strength decreased at 14 days and increased at 28 days. Mix B and Mix C became more brittle at 28 days. Result are summarized in Table 6.

Table 6. Stress and strain during curing time.

Mix	Cure Length (days)	Max Stress (psi)	Strain at Break (%)
A	7	1007	0.01
	14	1372	0.01
	28	1226	0.01
B	7	918	0.02
	14	834	0.02
	28	998	0.00
C	7	633	0.01
	14	847	0.01
	28	759	0.00

3.1.8 Compressive strength

Table 7 summarizes composition and compressive strength development over time.

Table 7. Material composition and compressive strength of developed mixtures.

Mix ID	Deionized Water	METSO® Beads 2048 (Anhydrous)	Na-Sil 1.25 (Water Already Added)	Metastar 501 Metakaolin	Class F Fly Ash Jacksonville 2017	Grade 120 GGBFS	7-Day Compressive Strength	28-Day Compressive Strength
	Weight %						MPa (psi)	
A	29	10	0	15	25	21	9.4 (1,360)	27.4 (4,000)
B	25	10	0	0	32.5	32.5	35.8 (5,197)	50.5 (7,327)
C	27.4	0	22.1	26.5	0	23.9	17.3 (2,503)	41.5 (6,013)

Mix A and Mix B have rapid strength development, excellent compressive strength at 28 days, excellent flow, and reasonable setting time. Mix C is a standard mix that was used for comparison purposes (Davidovits 2008, p

231). The greater microstructural compaction imaged in Figure 10c may explain the faster and higher strength development of Mix B versus Mix A evident in the table.

3.2 Structural test results for rehabilitated ties

Full-scale prototype repairs were performed on five specimens of damaged ties obtained in the field. These specimens had been exposed to weathering and regular railroad loading at Fort Campbell. Flexural testing was performed on ties rehabilitated with the candidate mixes, and compression tests were performed on cured inorganic polymer mortar and concrete cubes.

3.2.1 Tie preparation

After the mix and reinforcement selection process had narrowed to two mixes with three different reinforcement schemes, five deteriorated ties were selected for testing. Ties were cut from a length of 8 ft, 6 in. to 8 ft in order to fit them inside the mold to hold them during pouring of geopolymer mixtures. The mold was constructed of wood nominal 2 x 4s with non-stick plastic lining and separators between each tie. Each tie was power washed and the interior cavities were cleared of debris caused by deterioration by using a water pressure washer and air blower. Photos of the specimens' condition are shown in Figure 14.

Figure 14. Damaged railroad ties before rehabilitation (continued to next page).

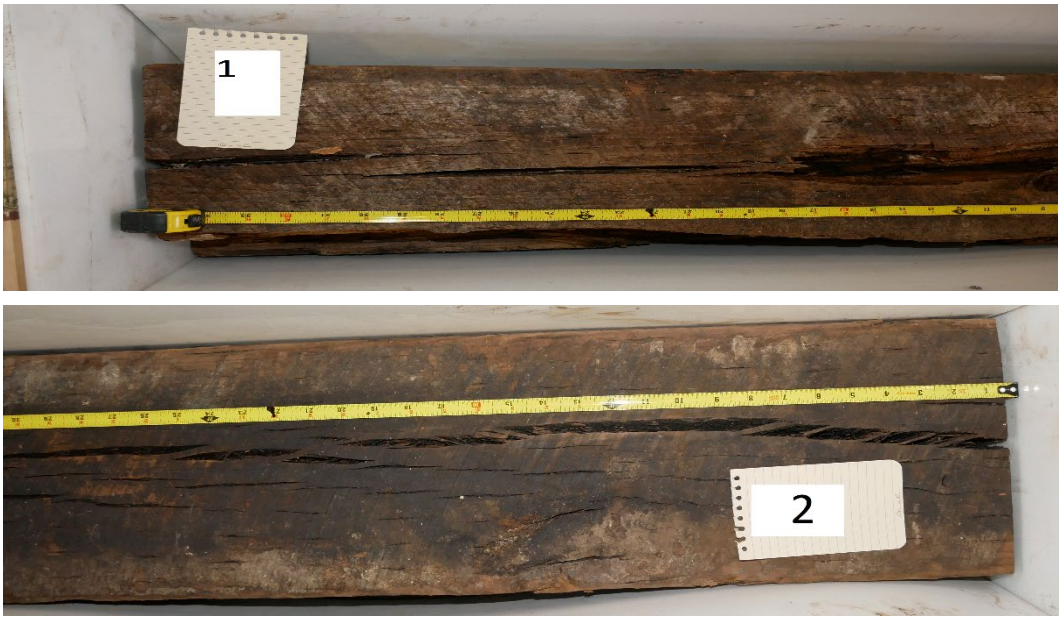

Figure 14 (concluded from previous page).

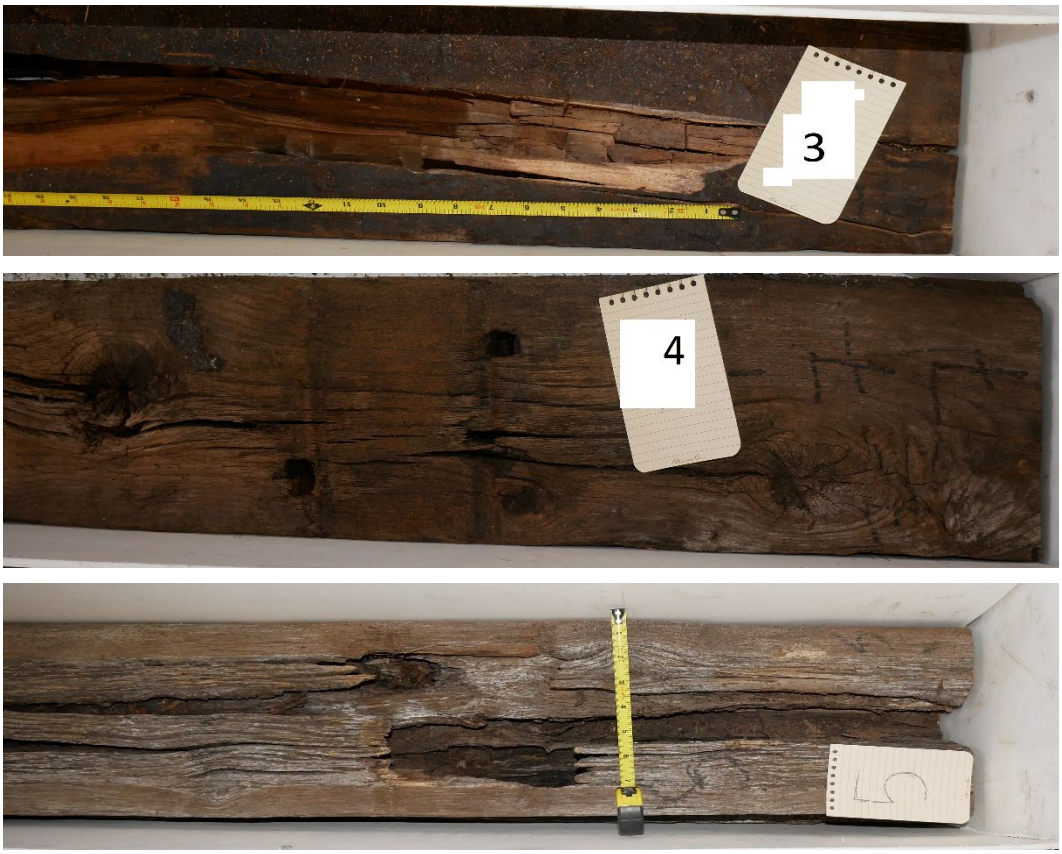

3.2.2 Flexural tests

Figure 15 shows the deformation specimen subjected to vertical loading. The support points are modeled as roller connections to eliminate friction and achieve accurate load measurements.

Figure 15. Undamaged tie under vertical load.

Figure 16 is the pretest position of rehabilitated tie #1, which was instrumented and ready for flexural testing.

Figure 16. Rehabilitated tie #1, before flexural testing.

Figure 17 is a rehabilitated tie subjected to load near failure.

Figure 17. Rehabilitated tie #1 after flexural loading.

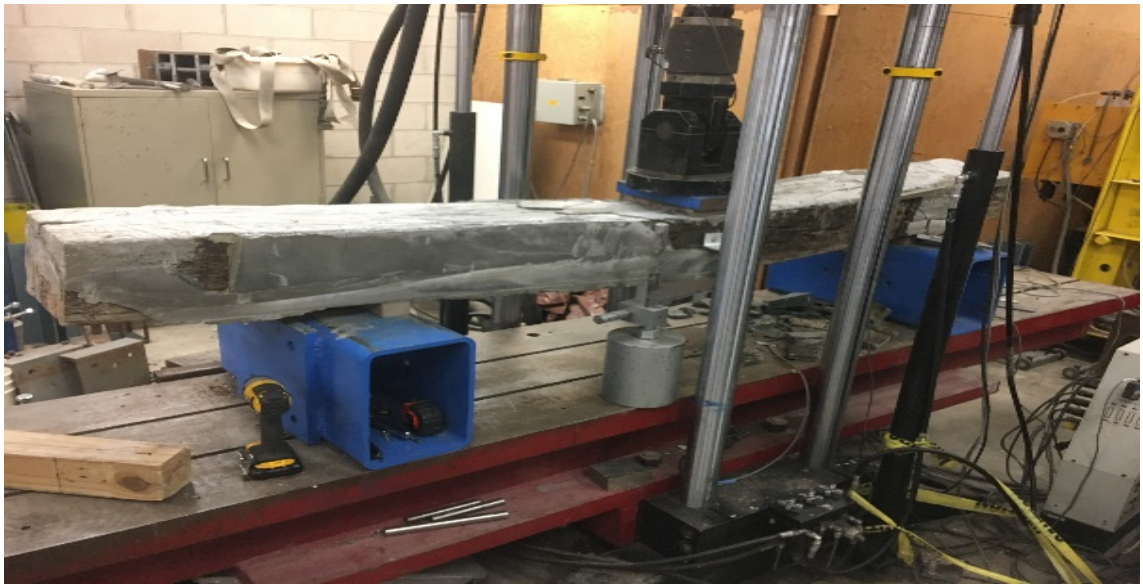

After testing all specimens in the manner above, each tie was cut at the center to determine how well the inorganic polymer had filled the void (Figure 18).

Figure 18. Cross section of post-tested tie #1–5 showing good penetration of inorganic polymer into wood.

Figure 19 shows the pretest position of rehabilitated tie #2 that is instrumented and ready for flexural testing.

Figure 19. Rehabilitated tie #2 before flexural testing.

Figure 20 shows post-test condition of rehabilitated tie #2, with longitudinal failure planes clearly visible.

Figure 20. Rehabilitated tie #2 after flexural testing.

Figure 21 is a pretest position of rehabilitated tie #5 instrumented and ready for testing.

Figure 21. Rehabilitated tie #5 before testing

Figure 22 shows a deformation of rehabilitated tie #5 subjected to vertical load.

Figure 22. Rehabilitated tie #5 after vertical load testing.

Figure 23–Figure 27 are load deflection curves for specimens #1–5. The x and y values represent the modulus of elasticity based on the measured data for each specimen.

Figure 23. Load-deflection of specimen #1.

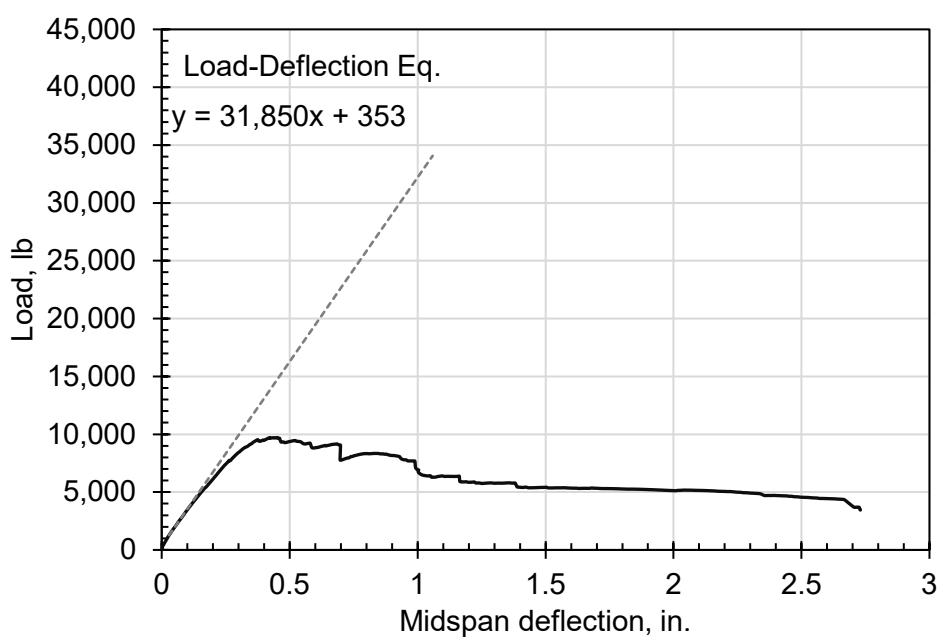

Figure 24. Load-deflection of specimen #2.

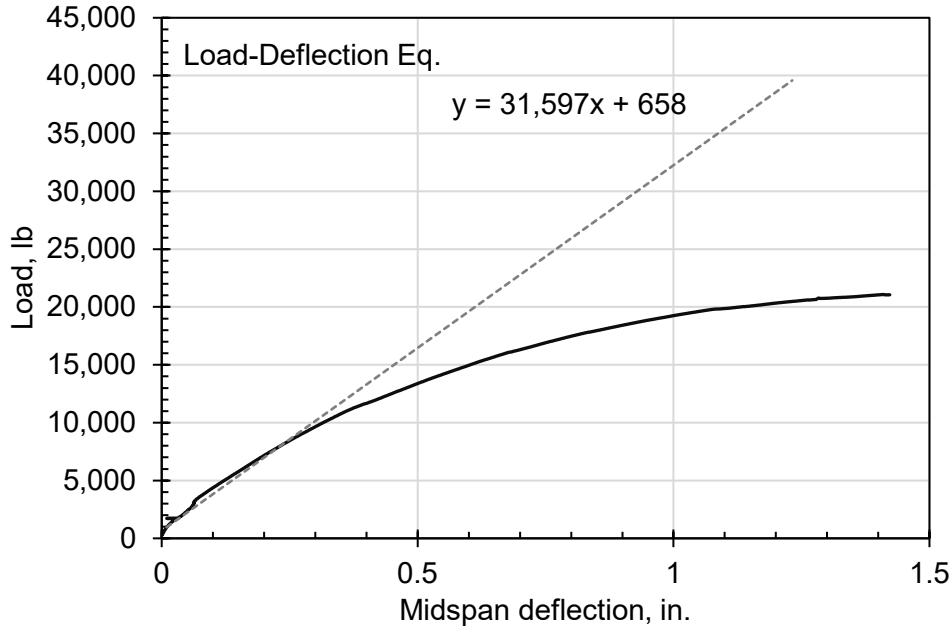

Figure 25. Load-deflection of specimen #3.

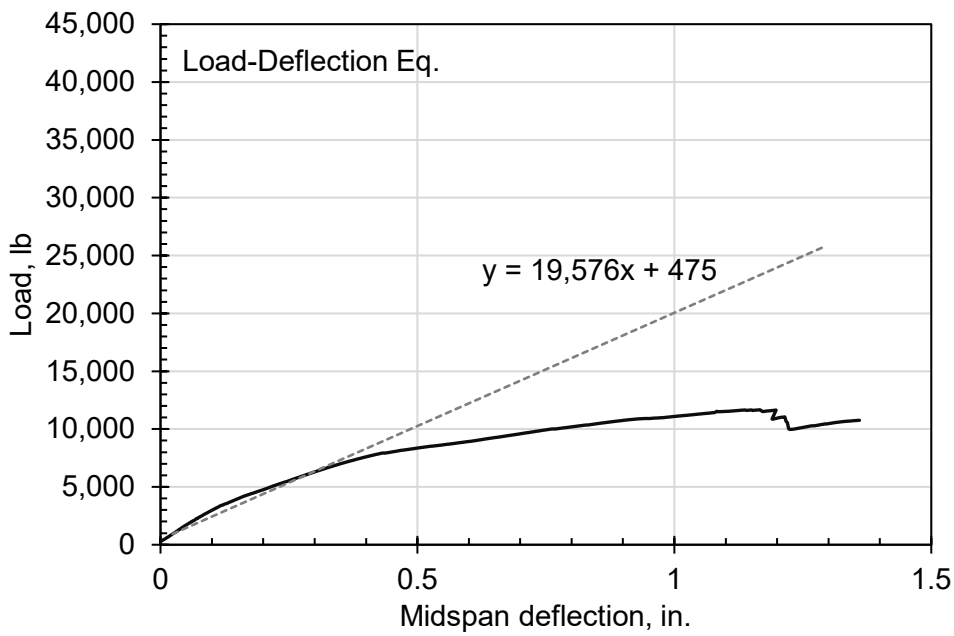

Figure 26. Load-deflection of specimen #4.

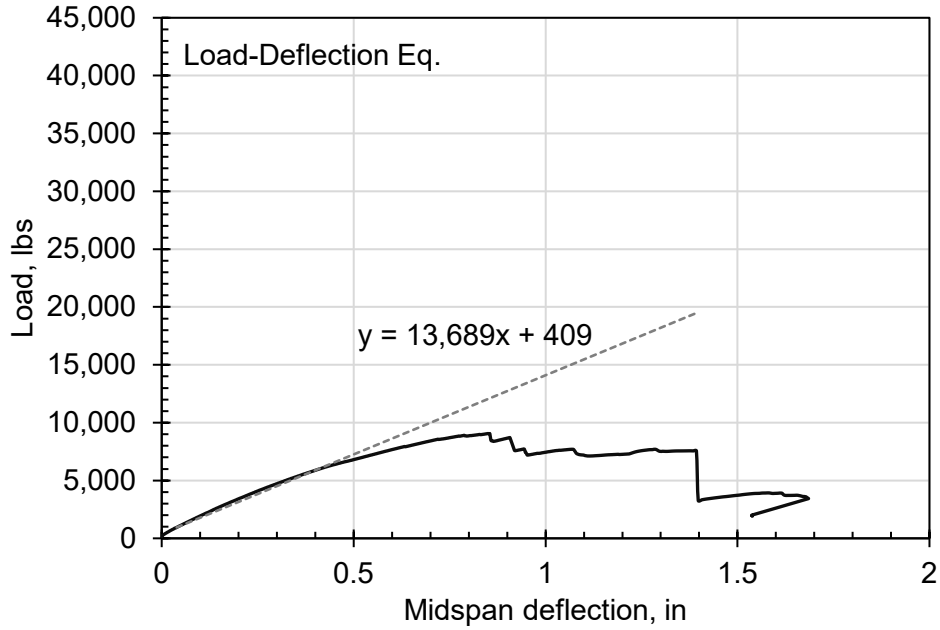

Figure 27. Load-deflection of specimen #5.

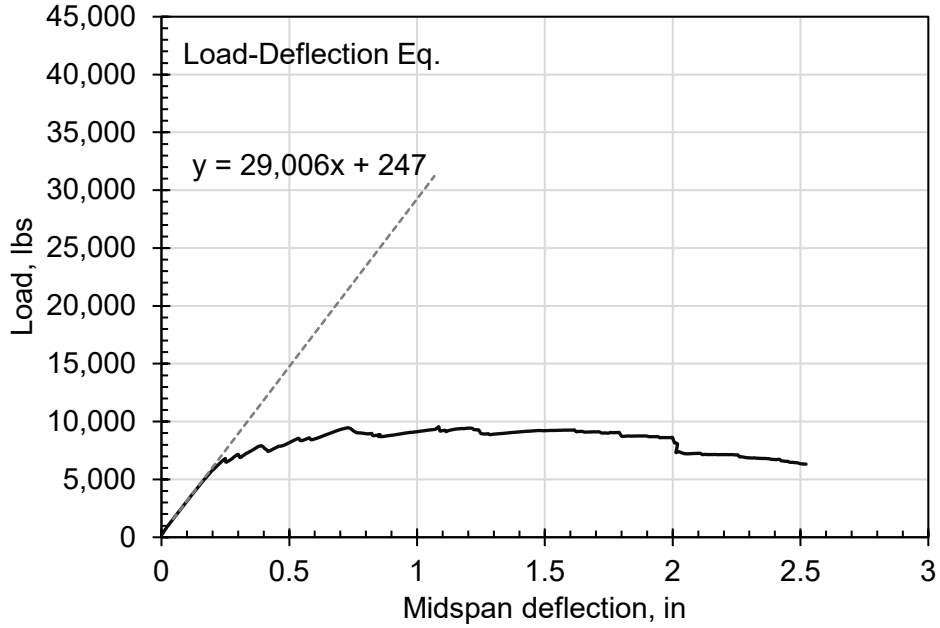

Figure 28 shows the load deflection curves of specimens 1–5. Figure 29 shows the load deflection curves of a new railroad tie and an aged but undamaged tie. Even without damage, older ties are expected to lose strength with time. The aged, undamaged tie was used as an average baseline to compare with rehabilitated ties.

Figure 28. Load vs deflection curves of rehabilitated ties #1–5.

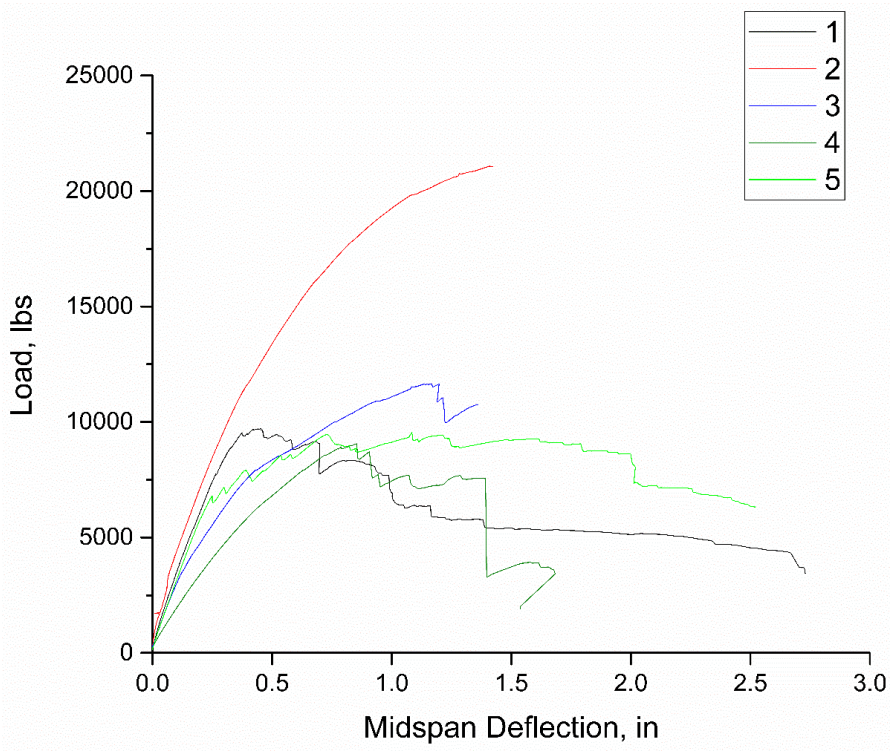

Figure 29. Load vs deflection curves of new and aged undamaged railroad ties.

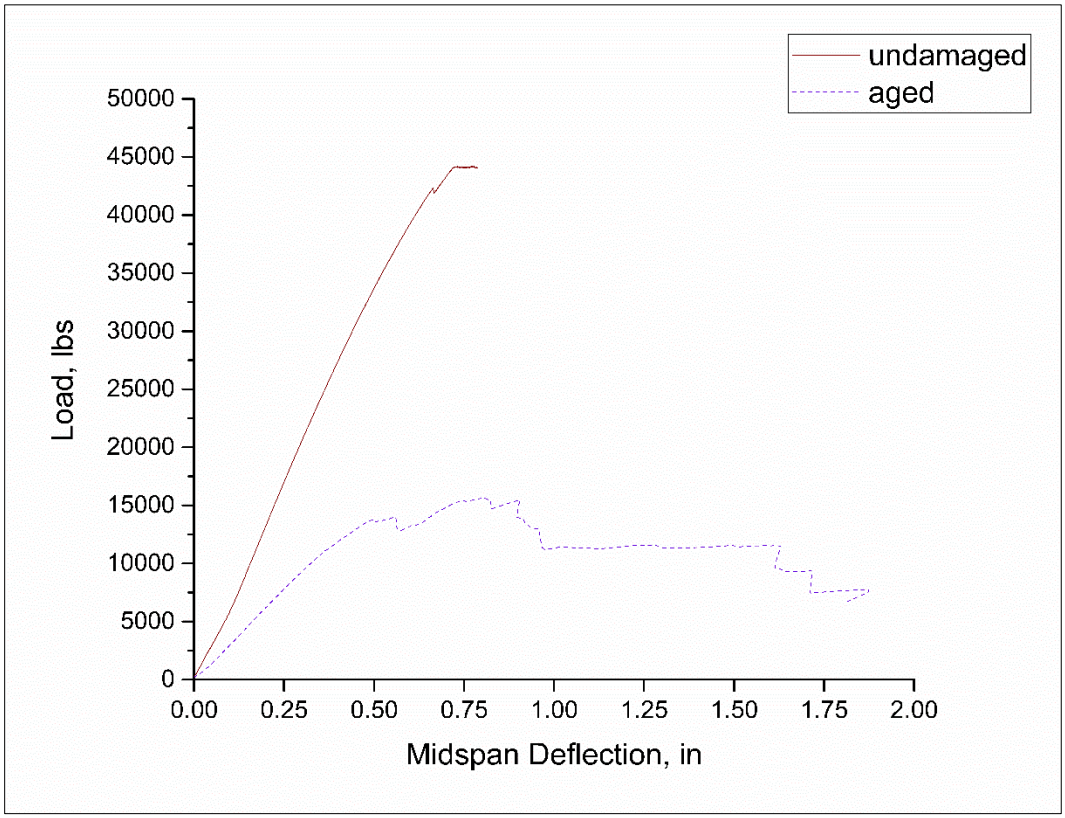

Figure 30 shows stress vs deflection curves of rehabilitated ties. Figure 31 shows stress vs deflection curves of new and aged, undamaged ties.

Figure 30. Stress vs deflection curves of rehabilitated ties #1–5.

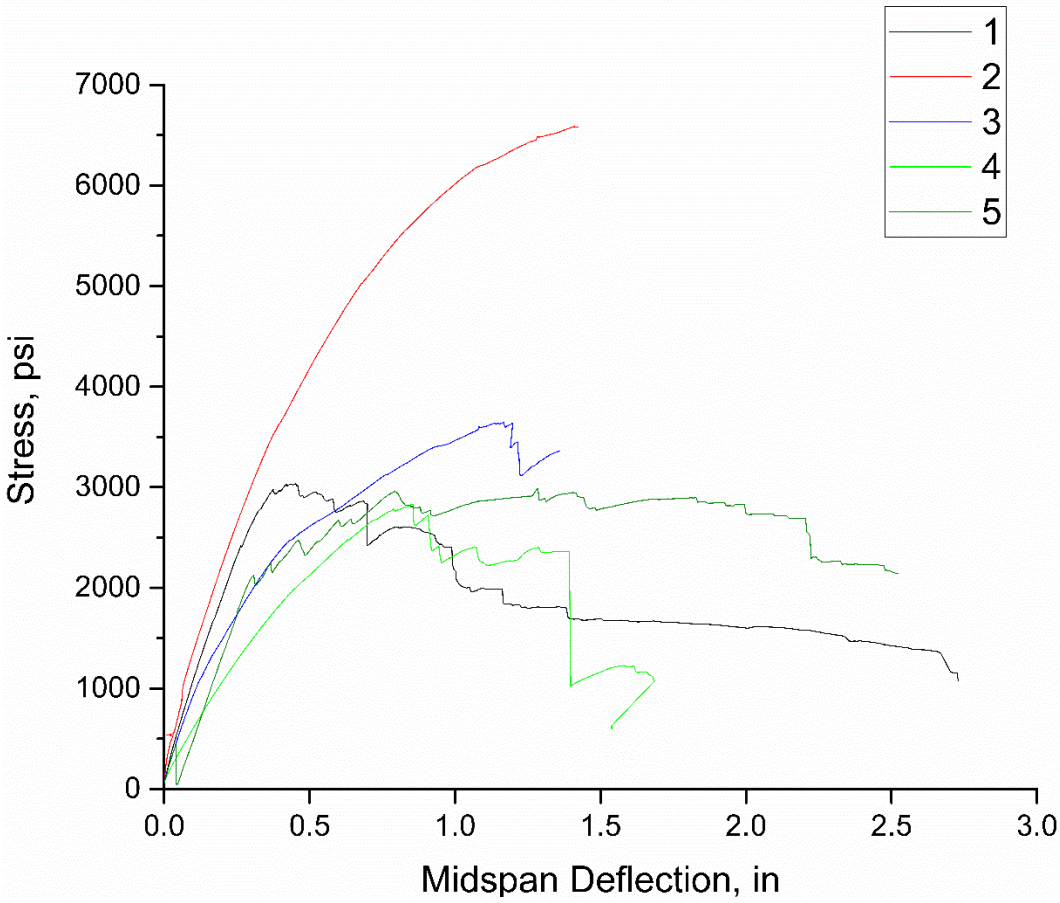

Figure 31. Stress vs deflection curves of damaged and undamaged railroad ties (only wood, no binder).

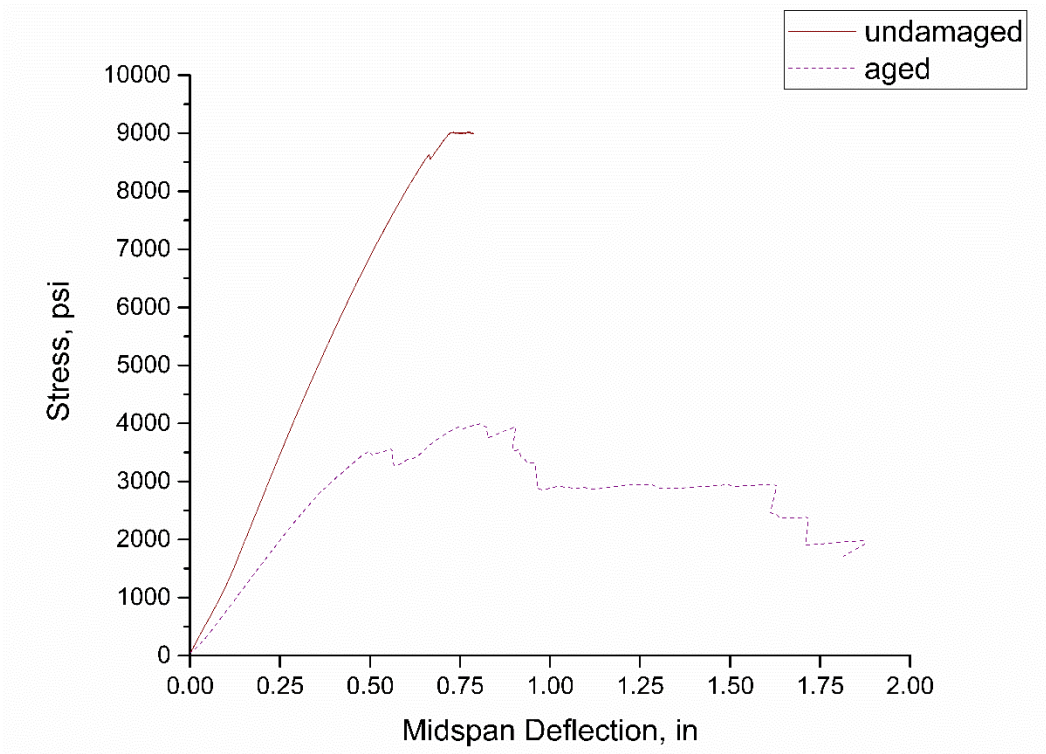

Maximum flexural stress, ultimate flexural strength, and the corresponding deflections are summarized in Table 8.

Table 8. Consolidated test data of rehabilitated railroad ties.

Tie number	Ultimate Load (lb)	Deflection at Ultimate Load (in.)	Ultimate Deflection at Failure (in.)	Maximum Flexural Stress (psi)
1	9716	0.45	2.73	3036
2	21080	1.41	1.42	6588
3	11661	1.17	1.36	3644
4	9055	0.85	1.69	2830
5	9563	1.08	2.52	2988
6 undamaged	44219	0.77	0.79	9024
7 - aged, undamaged	15667	0.81	1.81	3993

The weight of each tie was measured before and after casting with the inorganic polymer. Also, the moisture content of each tie was measured before casting. Both of these measurements are presented in Table 9. For further analysis such parameters can be useful. The inorganic polymer that was taken up by each tie can be calculated. If a void's shape inside the tie is known, a mathematical relationship can be developed to calculate the added strength of the rehabilitated ties that is due to the added inorganic polymer. (This calculation will be addressed in future work.)

Table 9. Rehabilitated railroad ties specifications.

Tie #	Weight Pre-Casting (lb)	Weight Post-Casting (lb)	Moisture Content (%)	Mix
1	159.5	338	13	49 Mortar
2	128	274	11 - 17	49 Cement
3	115.2	241	11 - 13	45 Mortar
4	81.6	217	5 - 8	45 Concrete
5	79	254	3 - 8	49 Concrete

Finally, the mix design for the rehabilitated ties are summarized in Table 10.

Table 10. Mass percent of mix components.

Tie #	Mix	Metso 2048	Water	Class F fly ash	Grade 120 slag	Metastar 501 MK	CERL sand in SSD condition	Sudaglass basalt 1/2 in. Unfluffed
1	B Mortar	0.10	0.25	0.33	0.33	0.00	0.00	0.00
2	B Binder	0.06	0.15	0.20	0.20	0.00	0.40	0.00
3	A Mortar	0.08	0.22	0.19	0.16	0.11	0.25	0.00
4	A Concrete	0.08	0.24	0.21	0.17	0.12	0.15	0.03
5	B Concrete	0.08	0.19	0.25	0.25	0.00	0.21	0.03

3.2.3 Compressive strength test

Results of strength tests on cube specimens from all mixes are shown in Table 11.

Table 11. Cube test results.

Tie #	Mix	Cure Length (days)	Average (psi)	Standard Deviation (psi)
1	B Mortar	14	5213	806
	B Binder	21	8152	605
4	A Concrete	7	2670	207
	B Concrete	14	3449	504
	A Concrete	29	1592	103
5	B Concrete	7	4113	576
	B Concrete	14	6628	150
	B Concrete	29	2882	379

3.3 Lessons learned

Grade 120 slag is finer than grade 100 slag, and its use contributes to faster set time and higher compressive strength. Metakaolin is a little more expensive due to calcination at higher temperatures, but its use results in more geopolymer formation. Metakaolin also requires more water to be present in the mix. Mix A is more viscous than Mix B. Filler phases like sand and basalt filaments increase the viscosity of the composites, but they contribute in toughening the final composite by deflecting cracks. The main reason for crack formation is due to dehydration, so it is important to seal the mixtures effectively with a water impermeable film and a wet towel (no contact between wet towel and binder) while it cures. This sealing step reduces drying shrinkage and ensures better chemical reaction in the binder.

Another lesson learned was that full-scale testing under real-world loading and trafficking is a complex and time-consuming process to coordinate with a railroad operator. This type of testing must be optimized for identifying good candidate ties, obtaining valid results and sufficient performance data, maintaining operational safety, and minimizing interruptions to train traffic. Thus, detailed preplanning and coordination are critical for such a study.

4 Economic Analysis

4.1 Costs and assumptions

The approximate cost per cubic yard for each binder that was evaluated is listed in Table 12. The cost of the slag and fly ash is largely driven by the distance to the material sources. The cost estimates for raw materials in the table do not include cost of transportation. Bulk quantity costs may also differ.

Table 12. Approximate cost of each binder mixture.

Mix ID	DI Water	Metso Anhydrous Beads 2048	Na-Sil 1.25 (water already added)	Metastar 501 Metakaolin	Class F Fly Ash Jacksonville 2017	Grade 120 GGBFS	Approx. Cost ($/yd³)	Compressive Strength in MPa (and psi)	
	Weight %							7-day	28-day
A	29	10	0	15	25	21	730	9.38 (1,360)	27.43 (4,000)
B	25	10	0	0	32.5	32.5	500	35.83 (5,197)	50.52 (7,327)
C	27.43	0	22.12	26.54	0	23.89	1051	17.26 (2,503)	41.45 (6,013)

Considering cost and performance, Mix B is the best and Mix A is the 2nd best. Mix C is not recommended. It is not only much more expensive than Mixes A and B, but testing showed that although the compressive strength of Mix C is good, the flexural strength is poor. The HCl and H_2SO_4 resistance of Mix C is also bad.

We will use $615 per cubic yard, the average of the costs of A and B, for the economic analysis.

The Army has approximately 1,900 miles of track. At AREMA-standard spacing, there are 3,249 ties per mile of track. This means the Army must maintain more than 6.1 million ties. An average life of a treated-wood tie is 30 years, and depending on service loads and environmental conditions,

service life can be much shorter. Assuming 5% of the ties are replaced each year, then the Army replaces about 310,000 ties annually.

4.1.1 Alternative 1 (commercially available crossties)

Currently, the Army does not rehabilitate damaged crossties; instead, it replaces them. A creosote-treated tie (which has an expected service life of 30 years) costs $75. The Army also uses engineered polymer composite ties to replace deteriorated wood ties. The composite tie has a minimum expected service life of 50 years and costs approximately $180. It costs $75 to cover transportation, labor to remove and dispose of the old tie, and to install a new tie. (This $75 cost also accounts for maintenance needed to the ballast after tie removal and reinstallation.) Because of the cost difference between wood and composite ties, we assume that twice as many ties are replaced with wood than with composite each year. Using these assumptions, replacement of 310,000 ties (205,000 with wood and 105,000 with composite) per year would cost the Army $57,525 thousand [205,000 x ($75 + $75) + 105,000 x ($180 + $75)].

The use of a combination of wood and composite ties reflects current practice, so the $57,525K is considered the baseline cost and is uniform over the 30 year return on investment analysis.

4.1.2 Alternative 2 (demonstrated technology)

It is estimated that about 14 ties can be treated with 1 yd^3 of inorganic polymer material resulting in a material cost of $44 per tie. The damaged ties must be cleaned with high pressure dry air before treatment. The cleaning and treatment procedure is estimated to cost $70 per tie. The total cost to rehabilitate a damaged tie is therefore $114.

Field surveys have shown that about half of the damaged ties are candidates for treatment, the others must be replaced.

An inorganic polymer-rehabilitated tie is expected to last for a minimum of 50 years so assume that the untreatable damaged wood ties are replaced with composite ties that also have a 50 year expected service life.

Using these assumptions, repair and replacement of 310,000 ties (155,000 repaired with an inorganic polymer and 155,000 replaced with composite)

per year would cost the Army $57,195 thousand [(155,000 x $114) + 155,000 x ($180 + $75)] annually.

4.2 Projected return on investment (ROI)

A return-on-investment (ROI) was calculated in accordance with OMB Circular A-94 (1992). This calculation is shown in Table 13. Because the first two years were dedicated to technology development the technology is assumed to not be utilized in the field until year 3, so the New System Costs are the same as the Baseline Costs for years 1 and 2.

The ROI is 5.47. This ROI value is based on current best practices, as well as projected maintenance and rehabilitation practices and costs.

Table 13. ROI calculation (values in thousands of dollars).

Return on Investment Calculation							
				Investment Required			640
				Return on Investment Ratio	5.47	Percent	547%
	Net Present Value of Costs and Benefits/Savings				710,312	713,810	3,498
A	B	C	D	E	F	G	H
Future Year	Baseline Costs	Baseline Benefits/Savings	New System Costs	New System Benefits/Savings	Present Value of Costs	Present Value of Savings	Total Present Value
1	57,525		57,525		53,763	53,763	
2	57,525		57,525		50,242	50,242	
3	57,525		57,195		46,688	46,958	269
4	57,525		57,195		43,634	43,886	252
5	57,525		57,195		40,780	41,015	235
6	57,525		57,195		38,109	38,329	220
7	57,525		57,195		35,615	35,821	205
8	57,525		57,195		33,287	33,480	192
9	57,525		57,195		31,108	31,288	179
10	57,525		57,195		29,072	29,240	168
11	57,525		57,195		27,173	27,330	157
12	57,525		57,195		25,395	25,541	147
13	57,525		57,195		23,736	23,873	137
14	57,525		57,195		22,180	22,308	128
15	57,525		57,195		20,727	20,847	120
16	57,525		57,195		19,372	19,484	112
17	57,525		57,195		18,108	18,212	104
18	57,525		57,195		16,924	17,022	98
19	57,525		57,195		15,814	15,906	91
20	57,525		57,195		14,779	14,864	85
21	57,525		57,195		13,813	13,892	80
22	57,525		57,195		12,909	12,983	74
23	57,525		57,195		12,062	12,132	70
24	57,525		57,195		11,273	11,338	65
25	57,525		57,195		10,535	10,596	61
26	57,525		57,195		9,849	9,906	57
27	57,525		57,195		9,203	9,256	53
28	57,525		57,195		8,602	8,652	50
29	57,525		57,195		8,042	8,088	46
30	57,525		57,195		7,515	7,559	43

5 Conclusions and Recommendations

5.1 Conclusions

This work produced the following accomplishments and observations:

- Two of the three binders (Mixes A and B) that were developed have good compressive and flexural strength, and reasonable costs.
- The two binders have good flow with a reasonable (and customizable) setting time at ambient temperature.
- The raw materials to make the two binders were carefully evaluated and selected based on physical properties, chemical properties, reasonable costs, easy availability, and overall feasibility.
- It was found that a variety of fillers (sand, basalt, chamotte) can be used.
- No new crystalline phases were formed on binders at early and late ages.
- Best practices for mixing and curing the binders were identified and documented, and they must be followed to ensure that each binder's properties turn out as predicted.
- To reduce excessive drying shrinkage, samples needed to be wrapped with plastic food-service film impermeable to water with a wet towel inside during curing.
- All binders (Mixes A, B, and C) exhibited reasonable resistance to chloride and shrinkage.

5.2 Recommendations

5.2.1 Applicability

This technique is potentially applicable to all modes of failure of wood ties, as discussed in section 3.2 of this report. Surface preparation is critical to the success of applying a synthetic polymer mix to repair damaged railroad ties. To effectively repair some ties, it may be necessary to enlarge the void, split, or areas around damaged portions of ties because decayed wood and foreign matter must be totally removed, using either mechanical tools or a high-pressure sprayer.

It is envisioned that a commercially available railroad cart could be modified and equipped with the necessary tools, a high-shear mixing machine, and space for the material components necessary to produce the required

blend and apply it as intended. This concept will be tested in future in situ validation testing (see section 5.2.3).

5.2.2 Implementation

This technology is not ready for DoD implementation at this time. After successful in situ field validation testing, this technology could be implemented DoD-wide for use on installation rail lines by appropriately modifying the following specification and technical criteria documents:

- Unified Facilities Guide Specification (UFGS) 34-11-00, *Railroad Track and Accessories*
- Technical Manual (TM) 5-628, *Railroads*
- Unified Facilities Criteria (UFC) 4-860-03, *Railroad Track Maintenance and Safety Standards*.

5.2.3 Future work

At the time of writing, the principal investigator was in discussions with personnel at McAlester Army Ammunition Plant in McAlester, Oklahoma, to identify several deteriorated ties in the installation's railroad network that would be suitable for demonstration of the in-place repair technology investigated in this project.

A prospective longer-term field validation study is envisioned that includes partnerships with McAlester Army Ammunition Plant, Fort Leonard Wood, Fort Campbell, and Crane Naval Depot. The focus of this work would be to develop a larger-scale plan for systematically rehabilitating decayed wood ties in place with minimal disruptions in railroad operations. In this future work, the rehabilitated ties would be subject to periodic monitoring, including instrumentation of all test ties. Data would be collected to establish a time-dependent stress/strain relationship. The result of this monitoring program would be quantitative measures of crosstie durability following rehabilitation.

References

Al-Chaar, Ghassan K., Peter B. Stynoski, Marion L. Banko, Kaushik Sankar, Waltraud M. Kriven, and Imad L. Al-Qadi. 2017. *Development and Testing of Geopolymers for Soil Stabilization on Military Installations*. ERDC-CERL TR-17-9. Champaign, IL: Engineer Research and Development Center, Construction Engineering Research Laboratory (ERDC-CERL).

AREMA. 2017. *Manual for Railway Engineering*. This four-volume manual is updated annually. Lanham, MD: American Railway Engineering and Maintenance-of-Way Association (AREMA).

ASTM C78. 2016. Standard Test Method for Flexural Strength of Concrete (Using Simple Beam with Third-Point Loading). West Conshohocken, PA: ASTM International.

ASTM C157. 2014. Standard Test Method for Length Change of Hardened Hydraulic-Cement Mortar and Concrete. West Conshohocken, PA: ASTM International.

ASTM C191. 2013. Standard Test Methods for Time of Setting of Hydraulic Cement by Vicat Needle. West Conshohocken, PA: ASTM International.

ASTM C293. 2016. Standard Test Method for Flexural Strength of Concrete (Using Simple Beam with Center-Point Loading). West Conshohocken, PA: ASTM International.

ASTM C267. 2012. Standard Test Methods for Chemical Resistance of Mortars, Grouts and Monolithic Surfacings, and Polymer Concretes. West Conshohocken, PA: ASTM International.

ASTM C403 / C403M-16, Standard Test Method for Time of Setting of Concrete Mixtures by Penetration Resistance. 2016. West Conshohocken, PA: ASTM International. www.astm.org

ASTM C1012 .2015. Standard Test Method for Length Change of Hydraulic-Cement Mortars Exposed to a Sulfate Solution. West Conshohocken, PA: ASTM International.

ASTM C1424-10. 2015. Standard Test Method for Monotonic Compressive Strength of Advanced Ceramics at Ambient Temperature. West Conshohocken, PA: ASTM International.

Bernal, Susan A., John L. Provis, Brant Walkley, Rackel San Nicolas, John D. Gehman, David G. Brice, Adam R. Kilcullen, Peter Duxson, and Jannie S.J. van Deventer. 2013. "Gel Nanostructure in Alkali-Activated Binders Based on Slag and Fly Ash, and Effects of Accelerated Carbonation." *Cement and Concrete Research* 53(Nov): 127–14.

Chung, Chul-Woo. 2010. "Ultrasonic Wave Reflection Measurements on Stiffening and Setting of Cement Paste. Doctoral thesis. Urbana, IL: Graduate College of the University of Illinois at Urbana-Champaign. Accessed 14 March 2019, http://hdl.handle.net/2142/15556

Chung, C., M. Mroczek, I. Park, and L.J. Struble. 2017. "On the Evaluation of Setting Time of Cement Paste Based on ASTM C403 Penetration Resistance Test." *Journal of Testing and Evaluation* 38(5): 527–533.

Davidovits, Joseph. 1982. "Mineral polymers and methods of making them." U.S. Patent Grant 1982-09-14. Washington, DC: U.S. Patent and Trademark Office.

——. 1991. "Geopolymers." *Journal of Thermal Analysis and Calorimetry* 37(8): 1633–1656.

——. 2008. *Geopolymer Chemistry and Applications*. Saint-Quentin, France: Geopolymer Institute.

——. 2013. "Geopolymer Cement: A Review." On file at Geopolymer Institute Library. Saint Quentin, France: Geopolymer Institute.

Davidovits, Joseph, Ralph Davidovits, and Marc Davidovits. 2012. Geopolymeric Cement Based on Fly Ash and Harmless to Use. CA2658117C, CA grant, French patent office, Paris.

Davidovits, Joseph, Maria Izquierdo, Xavier Querol, Diano Antennuci, Henk Nugteren, Valerie Butsellar-Orthlieb, Constantino Fernandez-Pereira, and Yolanda Luna. August 2014. *The Development of Room Temperature Hardening Slag / Fly Ash-Based Geopolymer Cements for Geopolymer Concretes*. Technical paper #22. The European Research Project GEOASH : (2004–2007). Saint-Quentin, France: Geopolymer Institute Library.

Duxson, P., A. Fernández-Jiménez, J.L. Provis, G.C. Lukey, A. Palomo, and J.S.J. Van Deventer. 2007 "Geopolymer Technology: The Current State of The Art." *Journal of Materials Science* 42(9): 2917–2933.

Ferdous, W., A. Manalo, A. Khennane, and O Kayali. 2015. "Geopolymer concrete-filled pultruded composite beams--concrete mix design and application." *Cem. Concr. Compos*. 58:1–13.

Kriven, Waltraud M. 2010. "Inorganic Polysialates or 'Geopolymers.'" American Ceramic Society Bulletin. 89(4): 31–34.

Kriven, Waltraud M., Jonathon L. Bell, and Matthew Gordon. 2003. "Microstructure and Microchemistry of Fully-Reacted Geopolymers and Geopolymer Matrix Composites." *Ceramic Transactions* 153: 227–250.

Musil, Sean S., Greg P. Kutyla, and Waltraud M. Kriven. 2012. "The Effect of Basalt Chopped Fiber Reinforcement on the Mechanical Properties of Potassium Based Geopolymer." In *Developments in Strategic Materials and Computational Design III: Ceramic Engineering and Science Proceedings*, p 31–42, presented at the 36th International Conference on Advanced Ceramics and Composites held 22–27 January, Daytona Beach, FL. Edited by Waltraud M. Kriven, Andrew L. Gyekenyesi, Gunnar Westin, Jingyang Wang, Michael Halbig, and Sanjay Mathur. Hoboken, NJ: John Wiley & Sons, Inc.

Musil, Sean S., and Waltraud M. Kriven. 2014. "Situ Mechanical Properties of Chamotte Particulate Reinforced, Potassium Geopolymer." *Journal of the American Ceramic Society* 97(3): 907–915.

OMB. 1992. *Guidelines and Discount Rates for Benefit-Cost Analysis of Federal Programs*. OMB Circular No. A-94. Washington, DC: Office of Management and Budget.

Puligilla, Sravanthi, and Paramita Mondal. 2013. "Cement and Concrete Research Role of Slag in Microstructural Development and Hardening of Fly Ash-Slag Geopolymer." *Cement and Concrete Research* 43(1): 70–80.

Ribero, Daniel, and Waltraud M. Kriven. 2016. "Properties of Geopolymer Composites Reinforced with Basalt Chopped Strand Mat or Woven Fabric." *Journal of American Ceramic Society* 99(4): 1192–1199.

Rill, E., D.R. Lowry, and W.M. Kriven. 2010. "Properties of Basalt Fiber Reinforced Geopolymer Composites." In *Strategic Materials and Computational Design: Ceramic Engineering and Science Proceedings*, Vol. 31. A collection of papers presented at the 34th International Conference on Advanced Ceramics and Composites held 24–29 January, Daytona Beach, FL. Edited by Waltraud M. Kriven, Yanchun Zhou, Miladin Radovic, Sanjay Mathur, and Tatsuki Ohji. Hoboken, NJ: John Wiley & Sons, Inc.

Rostami, H., and T. Silverstrim. 1996. "Chemically Activated Fly Ash (CAFA): A New Type of Fly Ash-Based Cement." In *Proceedings of the 13th International Pittsburgh Coal Conference*, p 1074–1079. Conference held 3–7 September 1996 in Pittsburg, PA. Red Hook, NY: Curran Associates, Inc.

Sankar, Kaushik, Ruy R.A. Sá Ribeiro, Marlene G. Sá Ribeiro, Waltraud M. Kriven, and P. Colombo. 2017. "Potassium-Based Geopolymer Composites Reinforced with Chopped Bamboo Fibers." *Journal of the American Ceramic Society* 100(1): 49–55.

Sindhunata, John L. Provis, Grant C. Lukey, Hua Xu, and Jannie S. J. van Deventer. 2006. "Effect of Curing Temperature and Silicate Concentration on Fly-Ash-Based Geopolymerization." *Industrial & Engineering Chemistry Research* 45(10): 3559–3568.

Suraneni, Pranoy, Sravanthi Puligilla, Eric H. Kim, Xu Chen, Leslie J. Struble, and Paramita Mondal. 2014. "Monitoring Setting of Geopolymers." *Advances in Civil Engineering Materials* 3(1): 177–192.

Yip, Ch. K., G.C. Lukey, and Jannie S.J. Van Deventer. 2005. "The Coexistence of Geopolymeric Gel and Calcium Silicate Hydrate at Early Stage of Alkaline Activation." *Cement and Concrete Research* 35(9): 1688–1697.

Zubrod, Rodney W. 2013 "Performance-Based Specification for Geopolymer Cement Binders and Supporting Laboratory Data," *Geopolymer Binder Systems*. STP 1566 STP1566. Leslie Struble and James K. Hicks, Eds., pp 165–184. doi:10.1520/STP156620120061. ASTM International: West Conshohocken, PA

REPORT DOCUMENTATION PAGE

Form Approved
OMB No. 0704-0188

Public reporting burden for this collection of information is estimated to average 1 hour per response, including the time for reviewing instructions, searching existing data sources, gathering and maintaining the data needed, and completing and reviewing this collection of information. Send comments regarding this burden estimate or any other aspect of this collection of information, including suggestions for reducing this burden to Department of Defense, Washington Headquarters Services, Directorate for Information Operations and Reports (0704-0188), 1215 Jefferson Davis Highway, Suite 1204, Arlington, VA 22202-4302. Respondents should be aware that notwithstanding any other provision of law, no person shall be subject to any penalty for failing to comply with a collection of information if it does not display a currently valid OMB control number. PLEASE DO NOT RETURN YOUR FORM TO THE ABOVE ADDRESS.

1. REPORT DATE (DD-MM-YYYY)
August 2019

2. REPORT TYPE
Final

3. DATES COVERED (From - To)

4. TITLE AND SUBTITLE
Rehabilitation of Deteriorated Wood Railroad Ties Using Inorganic Polymers: Final Report on Project F17-AR03

5a. CONTRACT NUMBER

5b. GRANT NUMBER

5c. PROGRAM ELEMENT NUMBER

6. AUTHOR(S)
Ghassan K. Al-Chaar, Kaushik Sankar, and Waltraud M. Kriven

5d. PROJECT NUMBER
CPC F17-AR03

5e. TASK NUMBER

5f. WORK UNIT NUMBER

7. PERFORMING ORGANIZATION NAME(S) AND ADDRESS(ES)
U.S. Army Engineer Research and Development Center (ERDC)
Construction Engineering Research Laboratory (CERL)
PO Box 9005
Champaign, IL 61826-9005

8. PERFORMING ORGANIZATION REPORT NUMBER
ERDC/CERL TR-19-15

9. SPONSORING / MONITORING AGENCY NAME(S) AND ADDRESS(ES)
Office of the Secretary of Defense (OUSD(A&S))
3090 Defense Pentagon
Washington, DC 20301-3090

10. SPONSOR/MONITOR'S ACRONYM(S)
OUSD(A&S)

11. SPONSOR/MONITOR'S REPORT NUMBER(S)

12. DISTRIBUTION / AVAILABILITY STATEMENT
Approved for public release. Distribution is unlimited.

13. SUPPLEMENTARY NOTES

14. ABSTRACT

The U.S. Army owns and maintains about 1,900 miles of railroad track configured as short lines for mission-required on military installations where ordnance and other heavy freight must be moved in quantity onsite, or to connect with the national railroad network for long-distance transport. Almost all of crossties used in these rail lines are made of creosote-treated wood to support the rails. Wood offers several advantages in terms of life-cycle costs and structural suitability. Chemical treatment of wood ties extends their life cycles, but service life is still finite due to rot, consumption by insects, and other stressors. The removal and replacement of failed wood ties is costly, time-consuming, and disruptive to rail operations. Furthermore, the residual preservative chemicals also create a costly disposal problem.

This report describes the development of a cementitious geopolymer material based on slag-fly ash binder mixtures formulated with properties making it suitable for use as a tough, affordable in situ tie-rehabilitation material. Two candidate formulations were validated in lab experiments as easy to prepare onsite, and demonstrating excellent flowability with good compressive and flexural strength. Field demonstrations are still required to validate rehabilitation procedures and performance characteristics in Army rail line operations.

15. SUBJECT TERMS
Railroads; Railroad ties--Maintenance and repair; Cement composites; Fly ash; Slag

16. SECURITY CLASSIFICATION OF:			17. LIMITATION OF ABSTRACT	18. NUMBER OF PAGES	19a. NAME OF RESPONSIBLE PERSON
a. REPORT	b. ABSTRACT	c. THIS PAGE			19b. TELEPHONE NUMBER (include area code)
Unclassified	Unclassified	Unclassified	UU	58	

Standard Form 298 (Rev. 8-98)
Prescribed by ANSI Std. 239.18